UCRL- 1231
c.2

UNIVERSITY OF CALIFORNIA — BERKELEY

TWO-WEEK LOAN COPY

This is a Library Circulating Copy
which may be borrowed for two weeks.
For a personal retention copy, call
Tech. Info. Division, Ext. 5545

RADIATION LABORATORY

UCRL 1231
c2

DISCLAIMER

This document was prepared as an account of work sponsored by the United States Government. While this document is believed to contain correct information, neither the United States Government nor any agency thereof, nor the Regents of the University of California, nor any of their employees, makes any warranty, express or implied, or assumes any legal responsibility for the accuracy, completeness, or usefulness of any information, apparatus, product, or process disclosed, or represents that its use would not infringe privately owned rights. Reference herein to any specific commercial product, process, or service by its trade name, trademark, manufacturer, or otherwise, does not necessarily constitute or imply its endorsement, recommendation, or favoring by the United States Government or any agency thereof, or the Regents of the University of California. The views and opinions of authors expressed herein do not necessarily state or reflect those of the United States Government or any agency thereof or the Regents of the University of California.

UNCLASSIFIED

UCRL-1231
Cy. 2

CRYSTAL STRUCTURES OF LANTHANIDE AND ACTINIDE BORIDES AND FLUORIDES

by

Allan Zalkin
B.S. (University of California at Los Angeles) 1948

DISSERTATION

Submitted in partial satisfaction of the requirements for the degree of

DOCTOR OF PHILOSOPHY

in

Chemistry

in the

GRADUATE DIVISION

of the

UNIVERSITY OF CALIFORNIA

Approved:

.....

.....

.....
Committee in charge

Deposited in the University Library.....
Date Librarian

TABLE OF CONTENTS

	page
ABSTRACT	3
CHAPTER I. THE CRYSTAL STRUCTURES OF CeB_4, ThB_4, AND UB_4	4
I. INTRODUCTION	4
II. PATTERSON PROJECTIONS	5
III. CORRECTION FOR ABSORPTION	8
IV. BORON POSITIONS	10
V. POWDER DIFFRACTION INTENSITIES	19
CHAPTER II. CRYSTAL STRUCTURES OF YTTRIUM AND THE RARE EARTH TRIFLUORIDES	23
I. THE CRYSTAL STRUCTURE OF YF_3	23
A. Introduction	23
B. Preparation of Crystal	23
C. Unit Cell and Space Group	24
D. Trial Structures and Subsequent Projections	25
E. Density Section and Ionic Positions	32
F. Description of Structure and Structure Amplitude Agreement	36
II. THE RARE EARTH FLUORIDES	48
A. Introduction	48
B. Experimental (Preparation)	48
C. Experimental (Observations)	49
D. Data on the Orthorhombic Trifluoride Structures	54
E. The Hexagonal Rare Earth Trifluorides	69
F. Other Analogous RX_3 Structures	74
G. General Discussion of the Two Trifluoride Structures	75
H. Miscellaneous Non-trifluoride Compounds	78
ACKNOWLEDGMENT	83
REFERENCES	84

CRYSTAL STRUCTURES OF LANTHANIDE AND ACTINIDE BORIDES AND FLUORIDES

Allan Zalkin
Department of Chemistry and Radiation Laboratory
University of California, Berkeley, California

ABSTRACT

The crystal structures of the isostructural compounds CeB_4, ThB_4, and UB_4 have been deduced from x-ray diffraction patterns of powders of the three compounds and single crystals of ThB_4. The space group is D^5_{4h}-- P4/mbm. The metal atoms are situated in layers, each atom having five nearly equidistant neighbors in the layer. The boron atoms form a three-dimensional network, with most of them situated in the planes half-way between the metal layers. The environment of each boron is very similar to that in UB_2 or to that in ThB_6. The boron-boron distances range from 1.69 to 1.80 A in these crystals.

The crystal structure of orthorhombic yttrium trifluoride has been worked out completely from x-ray diffraction patterns of single crystals of yttrium trifluoride. The space group is D^{16}_{2h} Pnma. The yttrium ion positions have been determined by several electron density plots. The fluoride ion positions have been determined by both electron density plots and steric arguments. The acquired ion-ion distances are quite reasonable, the shortest F-F and Y-F distances being 2.55 A and 2.20 A, respectively.

Rare earth trifluorides isostructural with YF_3, SmF_3 through LuF_3, have been prepared and their lattice constants measured. The lattice constants form a regular set of numbers. SmF_3, EuF_3, HoF_3, and TmF_3 were observed to be distructural having the hexagonal LaF_3 type structure as well as the orthorhombic YF_3 type structure. Cubic HoOF, and an unidentified hexagonal Na-Ho-F compound were observed and measured. A cubic ammonium-rare earth-fluoride compound observed in the preparation of erbium, holmium, and thulium trifluorides was measured, and was found to be analogous to the cubic YF_3 structure reported by Nowacki.

CHAPTER I

THE CRYSTAL STRUCTURES OF CeB_4, ThB_4, AND UB_4

I. INTRODUCTION

In an investigation of refractory borides (Brewer, Sawyer, Templeton, and Dauben, 1951) it was found that cerium, thorium, and uranium form isostructural tetraborides. The determination of this structure is described in the present paper. The existence and composition of the compound UB_4 were established by Andrieux (1929). Bertaut and Blum (1949) found the unit cell dimensions, space group, and uranium positions of UB_4, in independent agreement with our results. Blum has communicated privately that they also agree with our boron positions, found by steric considerations. A brief account of our results has appeared elsewhere (Zalkin and Templeton, 1949).

These borides were synthesized by heating the elements together in vacuum at about 1500°C. Most of the products were microcrystalline powders, but some thorium preparations contained clusters of single crystals a few tenths millimeter in size. These crystals were rectangular parallelepipeds, nearly cubic in habit, with very flat faces and sharp edges, and with black metallic luster.

Rotation, oscillation, and Weissenberg diffraction patterns, taken with copper K alpha x-rays, revealed the structure of these crystals to be tetragonal with the symmetry of the space group D^5_{4h}-- P4/mbm or of one of its subgroups. The powder patterns of CeB_4, ThB_4, and UB_4 were then indexed. The resulting lattice parameters (based on chromium $K\alpha_1$ = 2.2896 A) are listed in Table 1. The unit cell contains four molecules.

Table I. Lattice Parameters

	a	c	c/a	x-ray density
CeB_4	7.205 ± 0.008 A	4.090 ± 0.005 A	0.568	5.74 g/cm^2
ThB_4	7.256 ± 0.004	4.113 ± 0.002	0.567	8.45
UB_4	7.075 ± 0.004	3.979 ± 0.002	0.562	9.38[a]
UB_4[b]	7.066	3.97	0.562	

a Andrieux (1929) reports 9.32 as the experimental density.

b Bertaut and Blum (1949).

The faces of the ThB_4 crystals were of the forms {110} and {001}. The diffraction patterns were taken with rotation about the [110] and [001] axes, which are parallel to crystal edges.

II. PATTERSON PROJECTIONS

The intensities of the spots on the zero-layer Weissenberg photographs were estimated by visual comparison with a set of standard spots made by variable exposure time. The resulting data, with no correction for absorption, were used to compute projections of the Patterson function, shown in Figures 1 and 2. It is apparent from Figure 1 that the thorium atoms lie in a plane y = constant. We have chosen the origin so that y = 0 for these atoms. The same conclusion follows from the fact that the intensity of the reflection (hkl) is nearly independent of l, though this fact was at first obscured by the large absorption effects.

Only one arrangement of four thorium atoms in a plane was found to be congruous with the largest peaks in Figure 2. This arrangement is represented by:

4 Th in 4(g) of P4/mbm: $\pm$ ($\underline{u}$, 1/2+$\underline{u}$, 0; 1/2-$\underline{u}$, $\underline{u}$, 0)

$\underline{u} \cong 5/16$

A choice of $\underline{u} \cong 3/16$ gives the same structure, but with different origin.

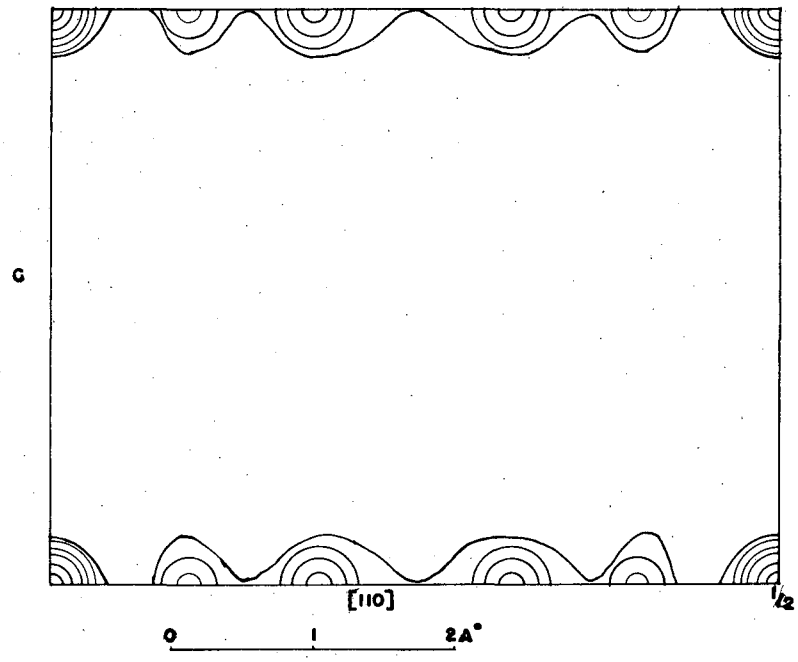

Fig. 1

The Patterson projection of ThB_4 along the [110] axis. Contours are drawn on an arbitrary scale and commence at 100, and continue up in units of 100 per contour.

MU 987

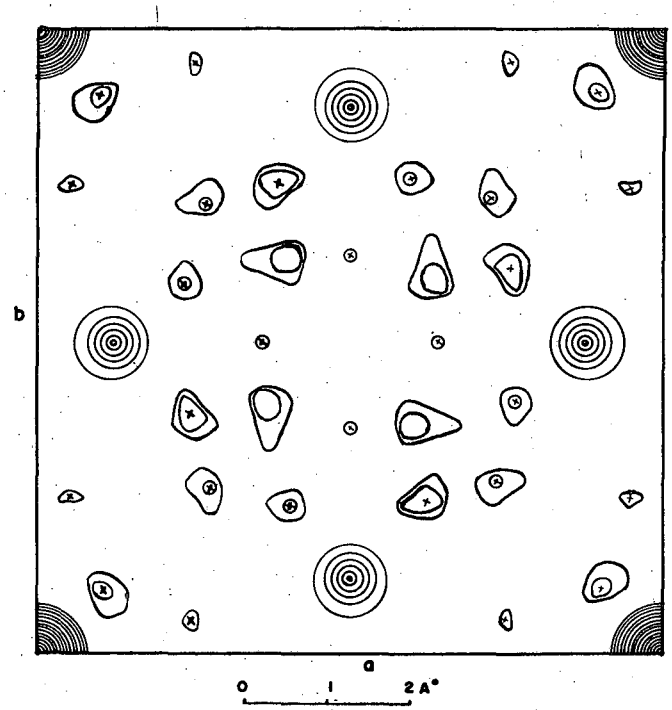

Fig. 2

The Patterson projection of ThB_4 on 001. Contours are drawn on an arbitrary scale, commencing at 50 with other contours drawn at intervals of 50 units. The crosses indicate those peaks which are extraneous and which disappear upon the application of an absorption correction.

MU 988

The agreement of this structure with these Patterson projections is far from perfect, because of the neglect of absorption effects. In Figure 2, crosses indicate those peaks which are extraneous. If the parameter u is exactly 5/16 (0.3125), then the contribution of thorium to the reflection (hkl) is zero if $4h - k = 8n + 4$ or if $4k - h = 8n + 4$. No such reflection was observed with copper Kα x-rays. It is estimated from a consideration of the variation of calculated structure factors with u that the parameter must be 0.313 ± 0.002.

III. CORRECTION FOR ABSORPTION

The half-thickness for absorption of copper Kα x-rays in ThB_4 is estimated to be 3×10^{-4} cm, or one or two percent of the dimensions of the crystals used. Thus diffraction is observed only for those surfaces which are exposed to the incident beam. If we neglect edge and end effects, for the moment, then the diffracted beam is zero unless it emerges from the same surface.

In Figure 3 only face AB is effective for diffraction toward M, while both faces AB and AD are effective toward N. The diffraction intensity from one face for an equatorial reflection is:

$$I = Q \int \exp\left[-\sigma x(\operatorname{cosec} \alpha + \operatorname{cosec} \beta)\right] \, dV$$

where Q includes all factors except absorption and volume, σ is the linear absorption coefficient of the crystal, x is the distance of the volume element dV from the surface, and angles α and β are related to the Bragg angle θ and the rotation coordinate of the crystal ϕ by

$$\alpha = \phi - m\pi/2$$

$$\beta = 2\theta - \alpha$$

$$m = 0, 1, 2, \text{ or } 3$$

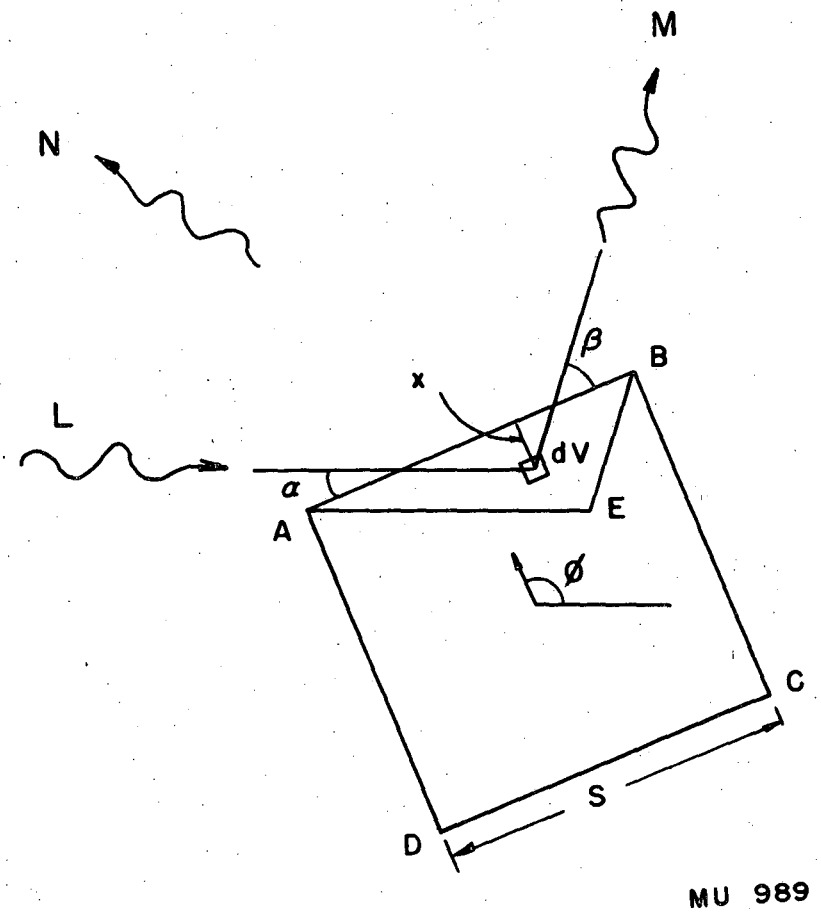

Fig. 3

and the integral is taken over the volume ABE. For a cube of side s large compared to $1/\sigma$, the result of the integration is

$$I = \frac{Qs^2}{(\text{cosec } \alpha + \text{cosec } \beta)}$$

The function $G = \sum(\text{cosec } \alpha + \text{cosec } \beta)^{-1}$, where all contributing faces are considered, is plotted as a function of ϕ and θ in Figure 4. The scale corresponds to that of the zero-layer Weissenberg photographs. To this function must be added the effect of edges and ends, which is difficult to calculate because it depends on the perfection of the form of the crystal. The sharper the edges, the less their contribution. We arbitrarily added 0.07 to G (10% of its maximum value) and found satisfactory agreement with the observed intensities. The constant factors s^2 and σ were omitted from the calculations.

The effect of these corrections is illustrated by Figure 5, which shows the results of summing the Patterson projection by the method of Huggins (1941), using the same data as in Figure 2 before and after correction.

Signs were calculated for F values, corresponding to the above structure for the thorium atoms. Projections of the electron density along [001] are shown in Figures 6 and 7. The accuracy of the data is not sufficient to resolve peaks due to boron, but the thorium parameter is well verified. Consequently, the boron atoms were located by space considerations.

IV. BORON POSITIONS

A large number of metallic borides are known in which a metallic lattice is interpenetrated by chains or nets of boron atoms. Each boron atom has from two to five boron neighbors, situated at a distance of 1.7 to 1.8 A; this distance is independent of the coordination number. Of particular interest to us here are the compounds AlB_2 (Hofmann and Jäniche, 1936),

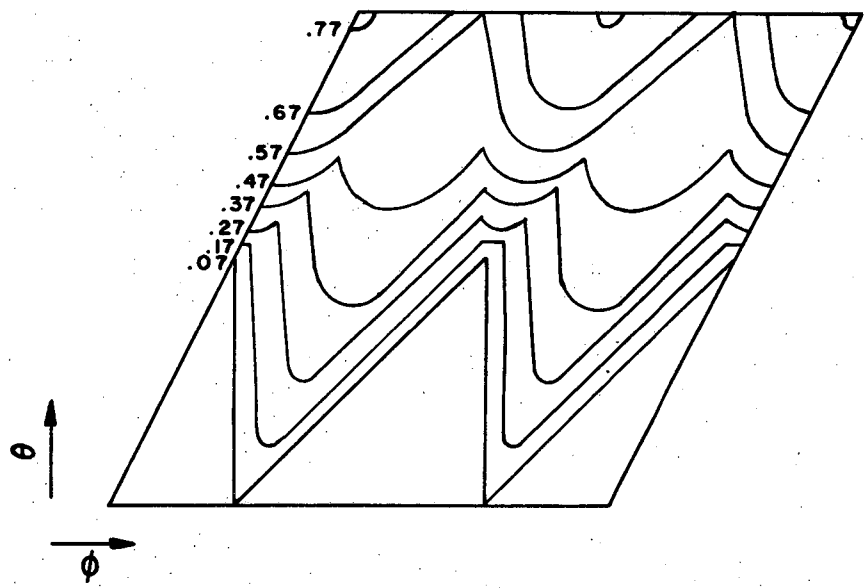

Fig. 4

Actual absorption correction mask used on the zero layer Weissenberg photograph along the 001 axis of ThB_4.

MU 990

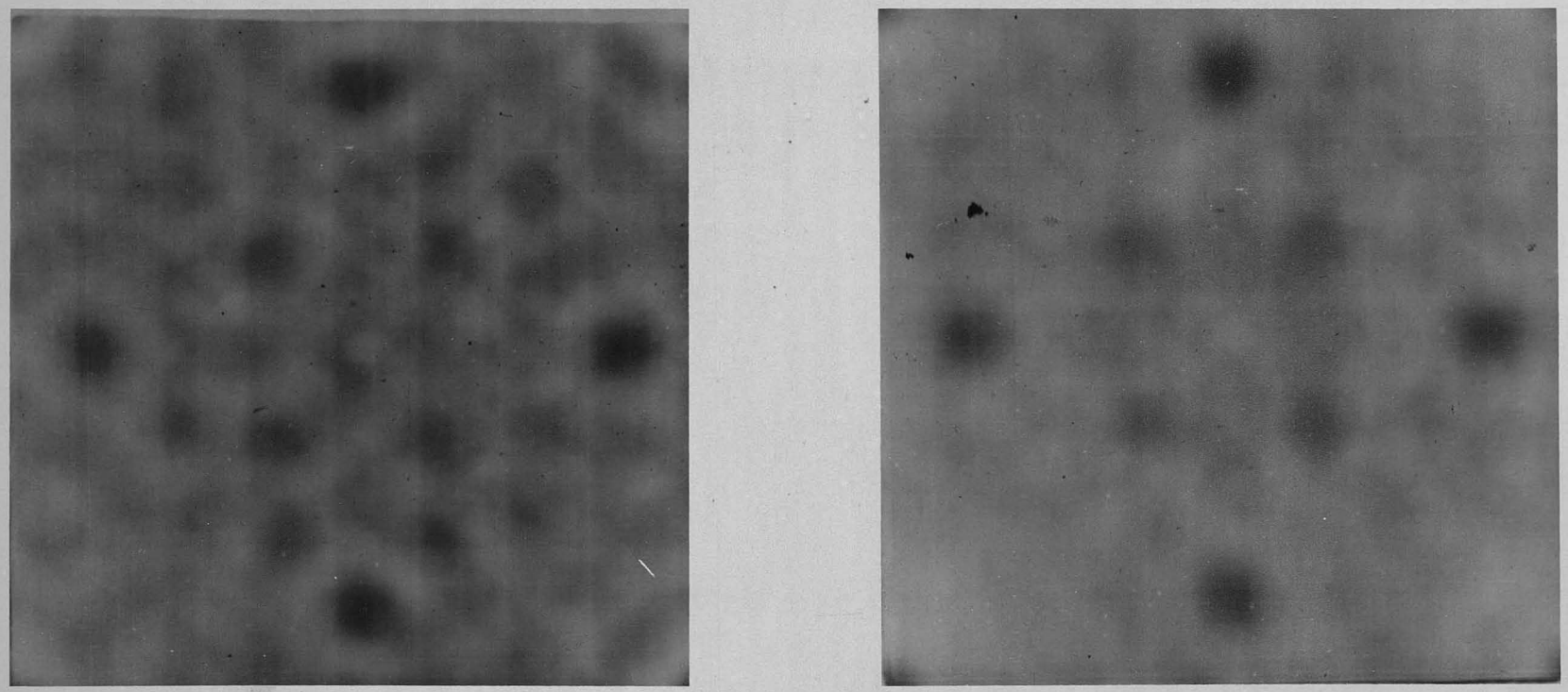

FIG. 5 THE PATTERSON PROJECTION OF ThB_4 ALONG THE 001 AXIS PREPARED WITH THE USE OF THE HIGGIN'S METHOD OF PHOTOGRAPHIC SUMMATION OF FOURIER SYNTHESIS. THE EFFECT OF THE ABSORPTION CORRECTION IS ILLUSTRATED HERE, THE LEFT AND RIGHT BEING THE UNCORRECTED AND CORRECTED PROJECTIONS, RESPECTIVELY.

OZ 988

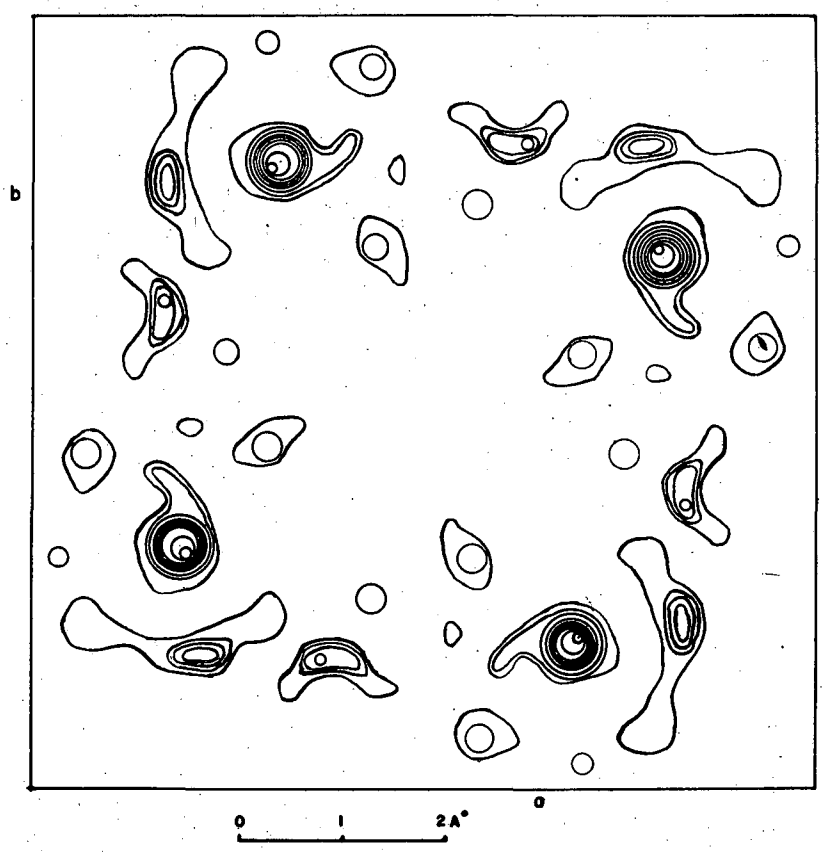

Fig. 6

(001) electron density projection. Uncorrected for absorption. Contours are drawn on an arbitrary scale commencing at 100 with contours at intervals of 100.

MU 991

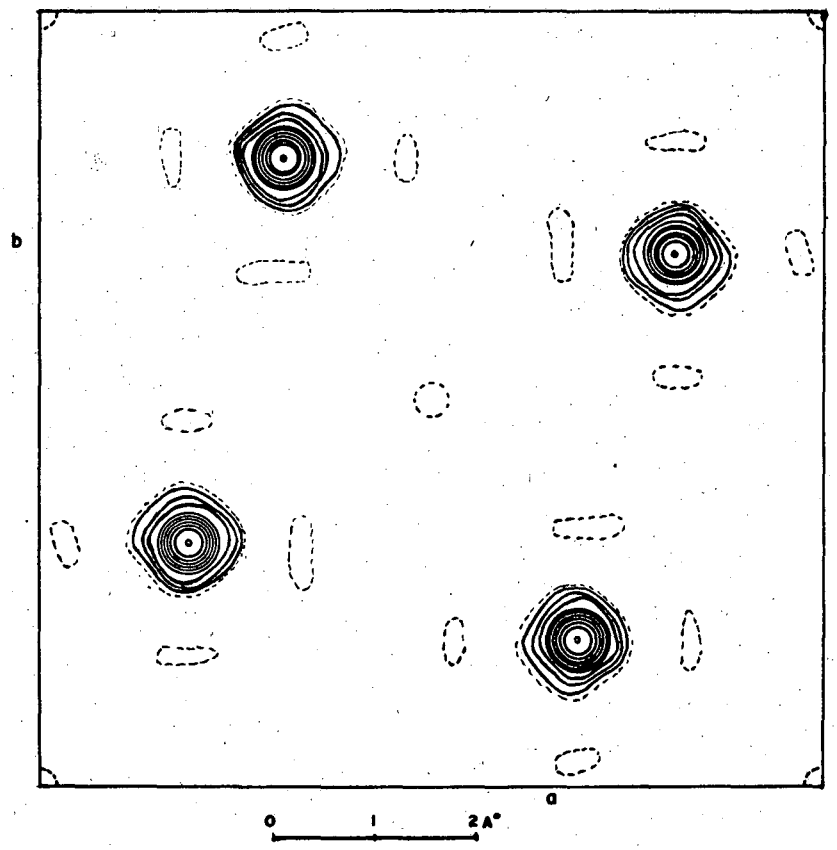

Fig. 7

(001) electron density projection, corrected for absorption. Contours are drawn on an arbitrary scale, commencing at 100 with contours at intervals of 100. The 50 contour has been indicated with a dotted line.

MU 992

ZrB_2 (McKenna, 1936), TiB_2 (Ehrlich, 1947), CrB_2, NbB_2, TaB_2 (Kiessling, 1949), VB_2 (Norton, Blumenthal and Sindeband, 1949), and UB_2 (Daane and Baenziger, 1949), in which a simple hexagonal metallic lattice is interpenetrated by boron sheets, and the compounds CaB_6, CeB_6, ThB_6, and others (Allard, 1932; v. Stackelberg and Neumann, 1932) in which a simple cubic lattice of metal atoms is interpenetrated by a three-dimensional net of boron atoms.

If the atoms are assigned radii consistent with those found in other borides, there is just room in ThB_4 for 16 boron atoms per unit cell, and these can be arranged in only one way. The thorium lattice consists of layers of the kind shown in Figure 8b, each thorium having five thorium neighbors in the same layer. Between the layers are holes each bounded by six thorium atoms arranged at the corners of a triangular prism, just as in UB_2, Figure 8a. There are other holes each bounded by eight thorium atoms at the corners of a square prism nearly the same size as the simple cube of ThB_6, one layer of which is shown in Figure 8c. One boron (called B II) fits into each triangular hole, just as in the MB_2 compounds, and there are four such holes per unit cell. There is room for an octahedron of six boron atoms (B I and B III) in each square hole, just as in ThB_6, and there are two of these holes per unit cell. The boron atoms in adjacent holes are in contact and form a continuous three-dimensional network. A layer of this network is shown in Figure 9. The octahedra are in contact with similar octahedra in adjacent layers.

The parameters of the boron atoms were calculated by trial and error to make the borons as nearly equidistant as possible and as far from thorium atoms as possible. The results are:

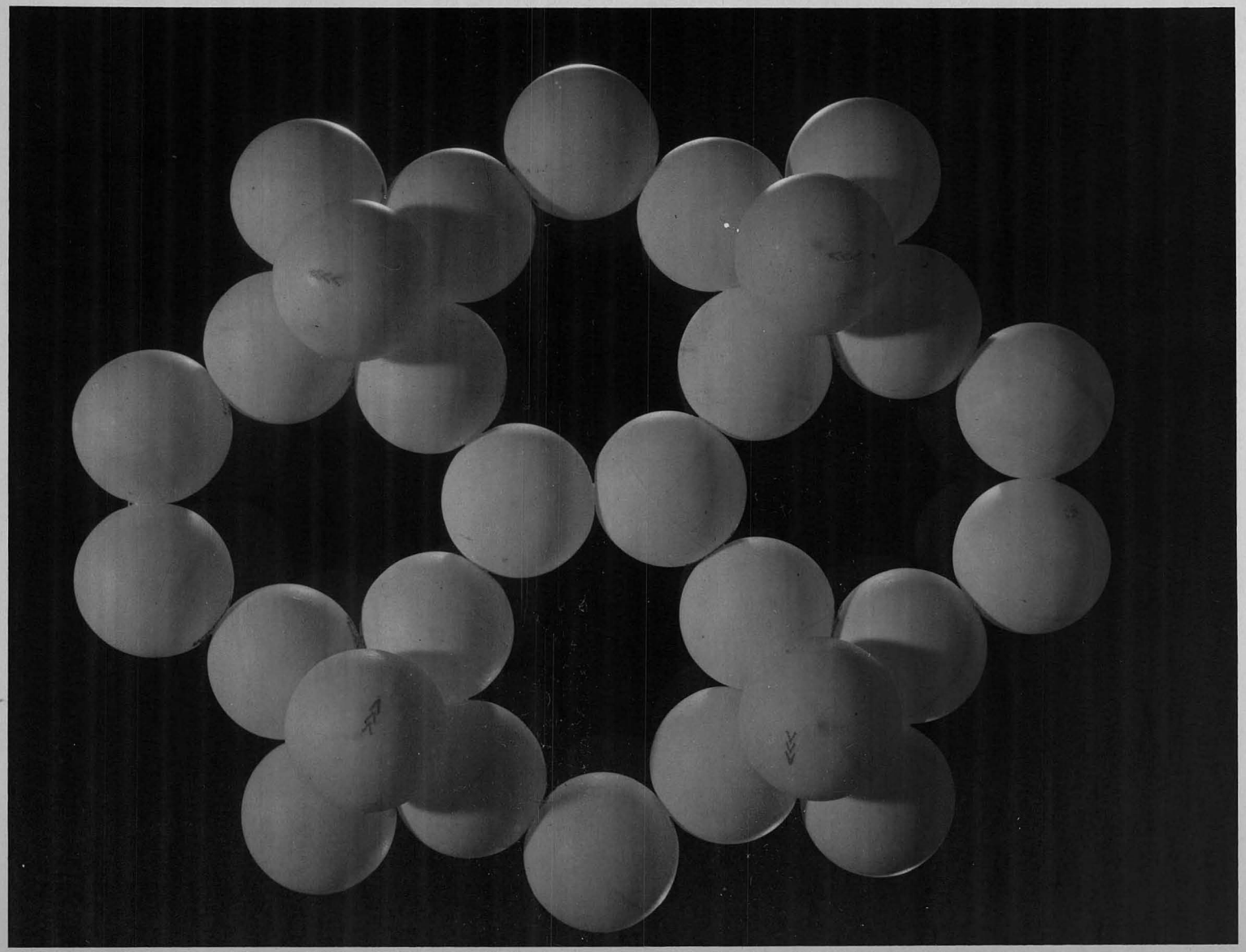

FIG. 9 THE MODEL OF THE BORON ARRANGEMENT IN ThB_4; THE Th BELONGS IN THE LARGE HOLES.

OZ 986

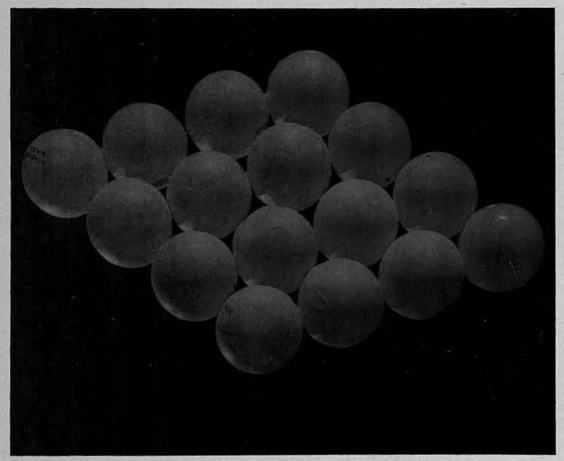

FIG. 8a MB_2

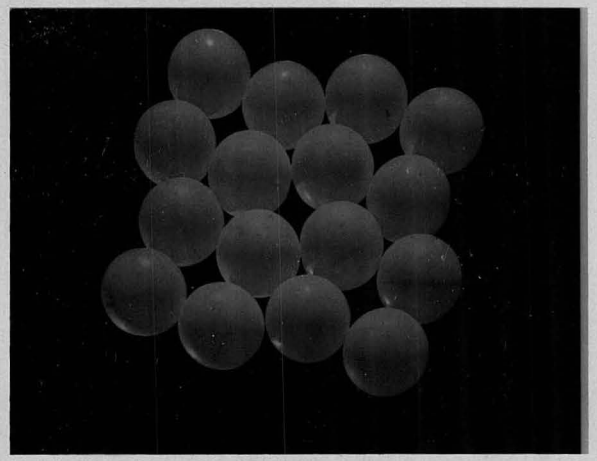

FIG. 8b MB_4

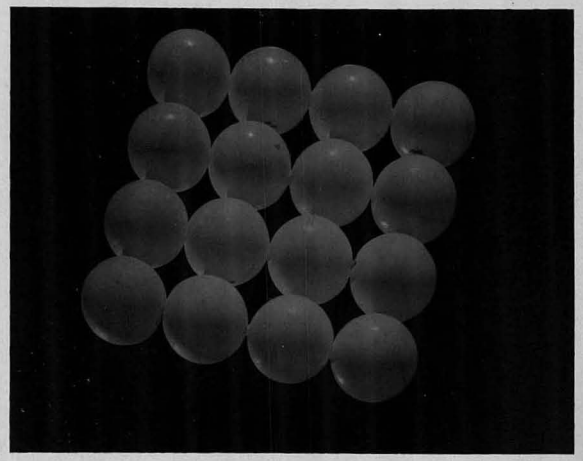

FIG. 8c MB_6

THESE MODELS ILLUSTRATE THE FACT THAT MB_4 HEAVY ATOM LATTICE IS INTERMEDIATE BETWEEN MB_2 AND MB_6 AS CAN BE EASILY SEEN ON COMPARING THE LARGE SQUARE HOLES OF MB_6 AND THE SMALL TRIANGULAR HOLES OF MB_2 BOTH OF WHICH ARE EXHIBITED IN MB_4.

OZ 987

4 B I in 4(e): $\pm(0,0,v;\ 1/2,\ 1/2,v)$

$v = 0.212$

4 B II in 4(h): $\pm(w,\ 1/2+w,1/2;\ 1/2-w,w,1/2)$

$w = 0.087$

8 B III in 8(j): $\pm(x,y,1/2;\ 1/2+x,1/2-y,1/2;$

$\bar{y},x,1/2;\ 1/2+y,1/2+x,1/2)$

$x = 0.170$

$y = 0.042$

The distances of nearest neighbors are:

	ThB_4	CeB_4	UB_4
B I - B I	1.74 A	1.73 A	1.69 A
- 4 B III	1.74	1.73	1.69
B II - B II	1.79	1.77	1.74
- 2 B III	1.79	1.78	1.75
B III- 2 B I	1.74	1.73	1.69
- B II	1.79	1.78	1.75
- 2 B III	1.80	1.78	1.75
M - 4 B I	2.78	2.77	2.71
- 4 B II	2.96	2.94	2.87
- 2 B II	3.10	3.08	3.01
- 8 B III	2.84	2.83	2.76
- 4 M	3.74	3.71	3.65
- M	3.85	3.82	3.75
- 2 M	4.11	4.09	3.98

V. POWDER DIFFRACTION INTENSITIES

The intensities of the diffractions lines of a powder of UB_4 were recorded with a Norelco diffraction apparatus equipped with a Geiger counter. These are tabulated in Table 1a, together with intensities calculated using the above parameters. The intensities calculated for the uranium atoms alone ~~is~~ are in reasonable agreement with those observed. Therefore we cannot say that the diffraction data determine the boron positions. However, there is observed some improvement of agreement when the boron atoms are included in the calculation.

The effect of boron on the intensities would be more significant in the case of CeB_4, but we did not have any samples of this compound pure enough and large enough for a spectrometer measurement.

Table 1a Intensity Calculations on UB_4

	$\sin^2\theta$*		Calculated Intensities		
hkl	calc.	obs.	not including borons	including borons	Observed Intensities
100	.0119		0	0	0
110	.0237		12	6	0
001	.0375	.0372	165	119	57
200	.0475	.0472	126	106	56
101	.0494		0	0	0
210	.0594	.0589	167	148	88
111	.0613		7	7	3
201	.0850	.0847	122	124	86
220	.0950		26	25	9

Table 1a Continued

hkℓ	$\sin^2\theta$* calc.	$\sin^2\theta$* obs.	Calculated Intensities not including borons	Calculated Intensities including borons	Observed Intensities
211	.0969	.0965	171	181	121
300	.1068		0	0	0
310	.1187	.1180	19	21	23
221	.1325	.1323	31	36	33
301	.1444		0	0	0
002	.1501	.1504	18	29	23
320	.1543		7	8	3
311	.1562	.1563	25	26	29
102	.1620		0	0	0
112	.1739		2	2	3
400	.1900		0	0	0
321	.1918	.1919	11	8	13
202	.1976	.1977	35	36	32
410	.2018	.2016	58	61	59
212	.2095	.2097	54	48	49
330	.2137	.2138	23	23	22
401	.2275		0	0	0
420	.2374		0	0	0
411	.2393	.2392	69	73	74
222	.2451	.2449	12	9	11
331	.2512	.2515	35	32	23
302	.2570		0	0	0
312	.2689	.2687	11	7	10

Table 1a Continued

hkℓ	$\sin^2\theta$* calc.	$\sin^2\theta$* obs.	Calculated Intensities not including borons	Calculated Intensities including borons	Observed Intensities
421	.2749		0	0	0
430	.2968	.2974	5^+	5^-	5
322	.3045	.3056	5^-	5^+	6
510	.3087		4	3	4
431	.3343	.3356	9	10	11
003	.3378		7	6	
402	.3401		0	0	0
520	.3443		2	2	<6
511	.3462	.3465	7	18	13
103	.3497		0	0	0
412	.3520	.3528	35	36	47
113	.3616		9	7	<7
332	.3638	.3645	19	22	20
440	.3800		0	0	0
521	.3818		4	3	3
203	.3853	.3855	12	12	19
422	.3876		0	0	0
213	.3972	.3972	19	20	19
530	.4036	.4037	16	17	17
441	.4174		0	0	0
600	.4274	.4278	5	5	10
223	.4328	.4338	5	5	7
610	.4393		8	8	<12
531	.4411	.4415	28	26	34

Table 1a Continued

hkℓ	$\sin^2\theta$* calc.	obs.	Calculated Intensities not including borons	including borons	Observed Intensities
303	.4447		0	0	0
432	.4469		6	5	9
512	.4558		5	5	<7
313	.4565	.4579	5	5	10
601	.4649	.4658	9	9	9
620	.4749		4	4	3
611	.4767	.4773	15	15	11

*Cu Kα λ = 1.5418A

CHAPTER II

CRYSTAL STRUCTURES OF YTTRIUM AND THE RARE EARTH TRIFLUORIDES

I. THE CRYSTAL STRUCTURE OF YF_3

A. Introduction

In 1938 Nowacki reported the crystal structure of a cubic YF_3 from a sample he prepared by the aqueous precipitation of yttrium with sodium fluoride; he has never succeeded in reproducing this compound. We have reasons to believe that the cubic material he reported is in fact a sodium yttrium salt of some type; this is discussed more fully later. Nowacki also briefly mentioned a different trifluoride prepared by treating yttrium in solution with hydrofluoric acid which gave him complex powder patterns.

Samples of YF_3 and several other rare earth trifluorides were presented to us and they were observed to give similar powder patterns which could not be indexed on a cubic, tetragonal or hexagonal lattice. These materials had been prepared by passing dry hydrogen fluoride and hydrogen gases over the rare earth sesquioxides at an elevated temperature, 700°C.

B. Preparation of Crystal

Since powder methods failed, we set out to obtain single crystals; we took a few milligrams of YF_3 powder, placed it in a small platinum crucible, which in turn was placed in an alumina crucible and then mounted in a tungsten coil furnace. The loaded furnace was then placed into the vacuum apparatus and evacuated to a pressure of between 10^{-5} to 10^{-6} mm of mercury, and the current turned up until the temperature of the alumina crucible was 1400°C as determined with an optical pyrometer.

The temperature was then decreased to 1000°C at a rate of about 2° per minute, and then shut off. When the platinum crucible was cut open, many irregular single crystal fragments were found adhering to the sides, where the temperature of the platinum was no doubt highest.

C. Unit Cell and Space Group

One of these fragments was mounted along its long dimension and placed in the Weissenberg apparatus for single crystal investigation. The crystal was photographed with copper K alpha x-rays (λ = 1.5418 A). The crystal was properly aligned and the following photographs obtained: rotation, zero, first, second, and third layer line patterns. From these photographs it was deduced that the unit cell was orthorhombic with the following dimensions:

a = 6.36 A b = 6.86 A c = 4.39 A.

The axis of rotation was the a axis. The following spots were obtained from the above films:

$$0k\ell,\ 1k\ell,\ 2k\ell,\ 3k\ell.$$

The following extinction rules were observed:

$$hk0 \qquad h = 2n$$

$$0k\ell \qquad k + \ell = 2n.$$

The above extinctions led to but one possible space group:

$$D_{2h}^{16} - Pnma.$$

Having but a fine powder and a few minute crystals unsuitable for specific gravity measurements, the number of atoms per unit cell was calculated without the experimental density ~~in a slightly different manner~~. Since Y and Sm were not too different in ionic radius, it was assumed that the molecular volume of

YF_3 in the orthorhombic cell was slightly smaller than SmF_3 in the known hexagonal cell. From the lattice parameters of SmF_3 and its cell content, we found 6 SmF_3 groups occupied 302 A^3, whereas the unit cell volume of YF_3 was 192 A^3, which yielded for the cell content of YF_3 something like 3.8 (the nearest integer of course being the wanted value, that being four yttrium fluorides per unit cell).

D. Trial Structures and Subsequent Projections

The yttriums ~~were~~ are much heavier in electron density than the fluorides and ~~were~~ are thus responsible for most of the diffraction; so as a first approximation, a trial structure was sought on the basis of the yttriums alone. Since there ~~were~~ are four yttriums per unit cell, they had to occupy one of the three four-fold positions available in the chosen space group Pnma, 4(a), 4(b), or 4(c). Both 4(a) and 4(b) required special extinctions which should appear here as systematic intensity variations with the following selection rules: $(hk\ell)$ strong only if $h + k + \ell = 2n$ and $k = 2n$. These were not observed, thus leaving the 4(c) positions as the only remaining alternative. These positions were:

$$x,1/4,z;\ \bar{x},3/4,\bar{z};\ 1/2 - x,3/4,1/2 + z;\ 1/2 + x,1/4,1/2 - z.$$

Our first big hint comes from the structure factor equation which for the 4(c) set and for the $0k\ell$ reflections ~~became~~ is:

$$A = 4 \cos^2 2\pi \left(\frac{k+\ell}{4}\right) \cos 2\pi\left(\frac{\ell}{4} + \ell z\right). \qquad (1)$$

Thus the yttrium contributions to the intensities of the $0k\ell$ set of reflections depend only on the z parameter. Upon perusal of the $0k\ell$ intensities on the zero layer, one peculiar set of extinctions was immediately evident. Of the $0k4$ spots permissible by the space group (004, 024,

044, and 064), only 044 was present, but even it was very weak. Thus for the intensities of these spots to be zero or very nearly so, A in Equation (1) must be zero and the second cosine factor on the right of the above equation must be zero. Now $\cos 2\pi(\ell/4 + \ell z) = 0$ when $\ell = 4$ if $z = 1/16$, $3/16$, $5/16$, etc., all of which yield the same result. The parameter $z = 1/16$ was used to check other intensities on the $0k\ell$ layer and found to give fair agreement considering the first approximation that we were neglecting the fluoride ion contributions. The intensities of all of the $0k\ell$ spots were then taken from the zero layer by measuring them visually using a comparison film strip with relative intensities 1, 2, 4, 8, 16, 32, 64, and 128. The intensities were corrected for polarization and Lorentz factors ~~using the formula:~~ with the following formula:

$$I_{hk\ell} \propto \left(\frac{1+\cos^2 2\theta}{\sin 2\theta}\right) F^2_{hk\ell} \qquad (2)$$

where I = intensity; F = structure amplitude; and θ = Bragg angle.

No absorption correction has even been attempted here because the crystal fragments available had such irregular shapes that little could be done about it.

The measured intensities were then used to obtain the series of $F_{0k\ell}$; the signs of the $F_{0k\ell}$ were determined by substituting $z = 1/16$ into Equation (~~2~~ 1). The electron density projection perpendicular to the a axis was then summed with the equation:

$$\rho(y,z) = \sum_k \sum_\ell F_{0k\ell} \cos 2\pi(ky+\ell z) \qquad (3)$$

Beevers-Lipson (1936) strips were used to ~~consummate~~ make the summations. The resulting summation is shown in Figure 10.

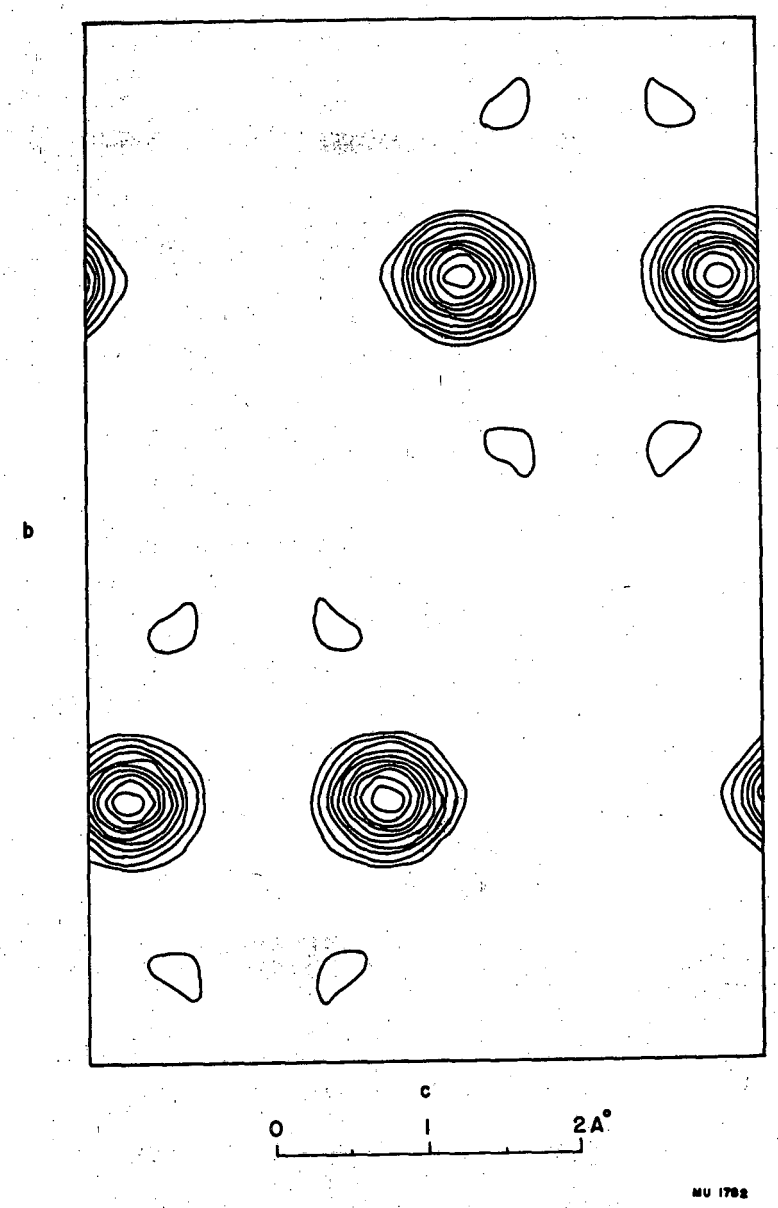

Fig. 10

The electron density projection of YF_3 along the a axis. Contours begin at +50 and increase at regular intervals of 50; the units of the contours are arbitrary. This projection utilizes nineteen independent non-zero terms. An independent non-zero term corresponds to each set of hkℓ values, i.e., hkℓ, $\bar{h}$kℓ, h$\bar{k}$ℓ, etc., since all of these terms have the same intensities.

The z parameter obtained from the above projection was z = 0.057 as compared with the trial value of z = 0.062. Resubstitution of z = 0.057 into Equation (2) did not give any changes in signs.

Another crystal fragment was mounted and by trial and error finally oriented along the c axis. Rotation, zero, first, and second layer photographs were obtained. The hk0 intensities were then measured and corrected in a similar manner as for the $0k\ell$.

It was then necessary to find a trial value for x to determine the signs for $F_{0k\ell}$. This was done by attempting to place the yttriums in the structure as equally spaced and uniformly as possible. A view of Figure 11 shows that in the (010) projection, the ions in the plane y = 1/4 were at a fixed distance with respect to each other independent of the value of x. Now the remaining thing to be done was to shift the rows in the two planes such that all of the ions are as uniformly spaced as possible.

The distances were best adjusted by choosing x = 3/8 (0.375) as our approximation. The c face density projection was then made (Figure 12), the signs for the F_{hk0} values being determined using x = 3/8, y = 1/4, and ℓ = 0. The equation for the density projection was:

$$\rho(xy) = \sum_h \sum_k F_{hk0} \cos 2\pi(hx+ky). \qquad (4)$$

The x parameter from the projection turned out to be 0.366 as compared to 0.375 used as the trial value.

Another crystal fragment was then oriented such that the axis of rotation was the b axis. The $h0\ell$ intensities were measured and the $F_{h0\ell}$ values obtained. The signs for the structure amplitude were calculated using x = 0.366, k = 0, and z = 0.057. Figure 13 is the b face electron density projection using the equation:

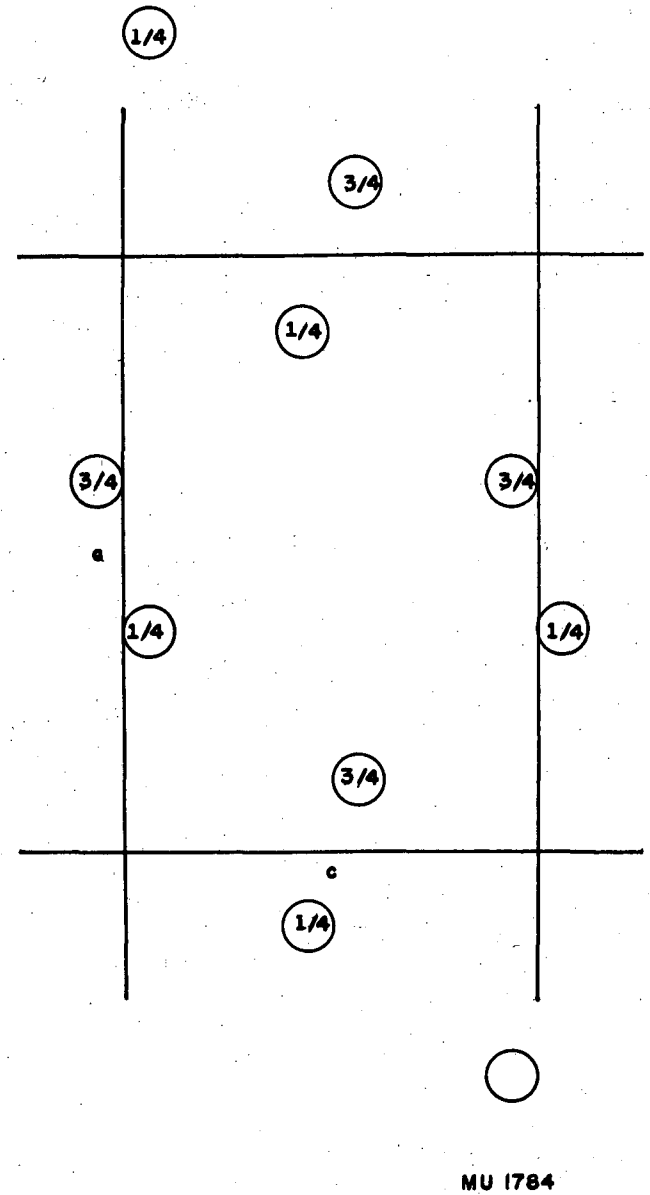

Fig. 11

The (010) projection of the yttriums in the trial structure.

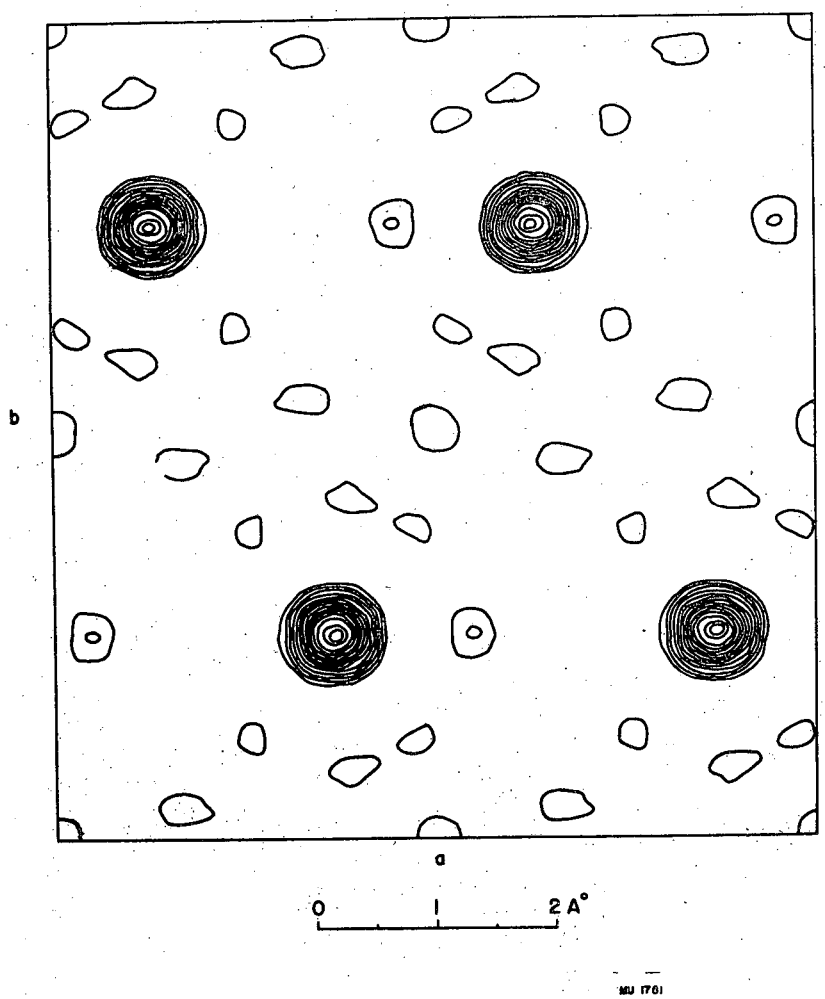

Fig. 12

The c face electron density projection for YF_3. Contours are in arbitrary units beginning at +50 and increasing in intervals of 50. Twenty-six non-zero independent intensities were used.

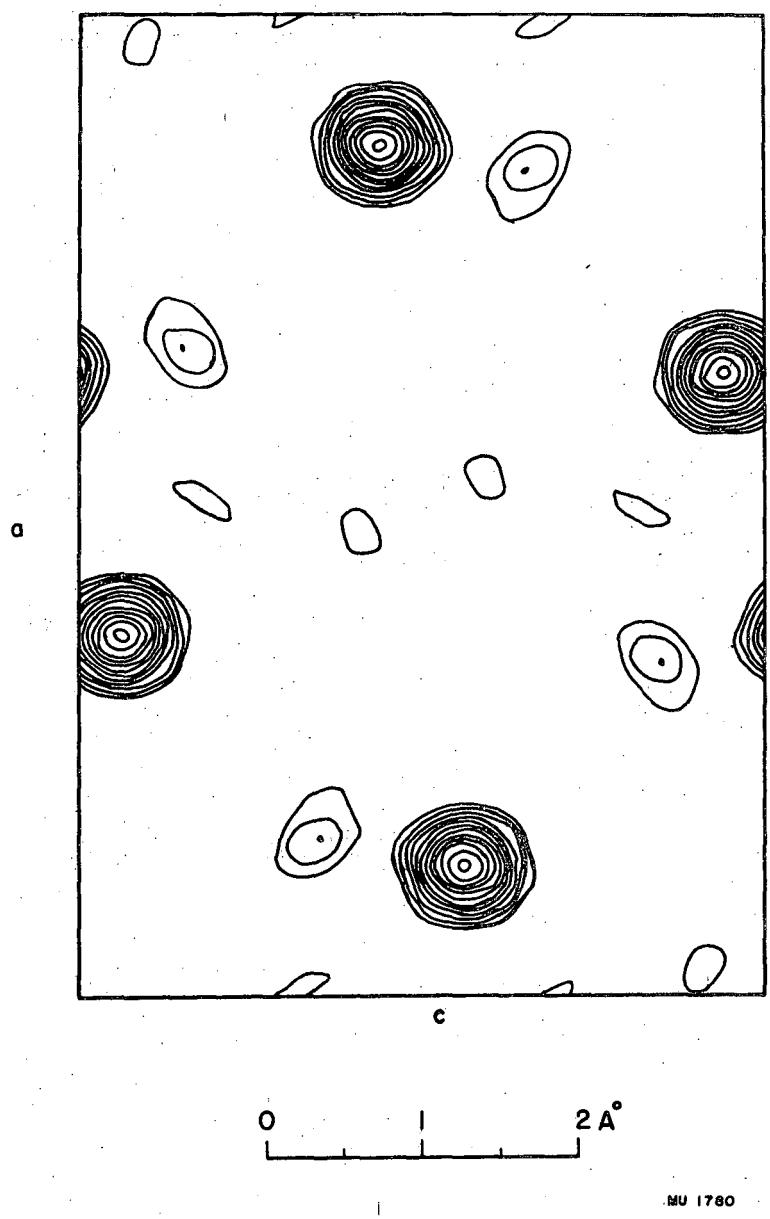

Fig. 13

The b face electron density projection for YF_3. Contours are in arbitrary units beginning at +50 and increasing intervals of 50. Twenty-nine non-zero independent terms were utilized.

$$\rho(xz) = \sum_h \sum_\ell F_{h0\ell} \cos 2\pi(hx+\ell z) \qquad (5)$$

The values of x and z obtained here were 0.368 and 0.053 as compared with the two previous values of 0.366 and 0.057.

E. Density Section and Ionic Positions

Yttrium Positions

In order to determine the x and z values more accurately, it was decided that an electron density section would have to be made through the plane y = 1/4. The available intensities were from ten layer line films with the following set of spots:

$0k\ell$	$h0\ell$	$hk0$
$1k\ell$	$h1\ell$	$hk1$
$2k\ell$	$h2\ell$	$hk2$
$3k\ell$		

The intensities of all of the above spots were measured and corrected for both polarization and velocity; the velocity correction values were those given by Tunnel (1939). The signs of the $F_{hk\ell}$ were calculated using x = 0.055 and z = 0.367. The above values for x and z were averages obtained in the three projections. The electron density section was made using the equation:

$$\rho(x\ 1/4\ z) = \sum_h \sum_k \sum_\ell F_{hk\ell} \cos 2\pi(hx + \frac{k}{4} + \ell z) \qquad (6)$$

The (040) section is shown in Figure 13.

The values obtained for x and z from the section were 0.366 and 0.059, and were assumed to be the best value except for a small correction to be made later on.

Fluoride Positions

It ~~We were~~ now was possible ~~in a position~~ to determine the position of the fluoride ions ~~. We were able to solve this problem~~ using geometrical and sterical arguments, with strong hints from their appearances in the electron density plots.

There were twelve fluoride ions in the unit cell which we found to occupy the one available eight fold position and the 4(c) four fold position; the space group has no twelve or higher fold position. The decision to start with this rather than with three four fold positions comes from the electron density plots and from spatial arguments. Let us see what the density projections showed us regarding the fluoride ions.

1. Figure 10 - a Projection.-- There exist~~s~~ in this projection eight small peaks interpretable as eight fold fluoride positions. The four fold ions apparently don't show up here at all.

2. Figure 12 - c Face Projection.-- Several small peaks show up, half of which are extraneous. The four larger ones are apparently the four fold fluoride ions and are situated at 1/4 along the b axis which would indicate it as being in a 4(c) set, like the yttriums, but of course with different parameters. The eight fold fluorides show up here also, but not a great deal more so than the general background peaks.

3. Figure 13 - b Face Projection.-- Here the eight fold fluorides show up quite well, because in this projection each of the +150 peaks present represents the projection of two eight fold fluoride ions in depth. The remaining peaks have no significance.

4. Figure 14 - (040) Section.-- The four fold fluoride ions appear clear of the eight fold ones, which are not positioned in this particular plane.

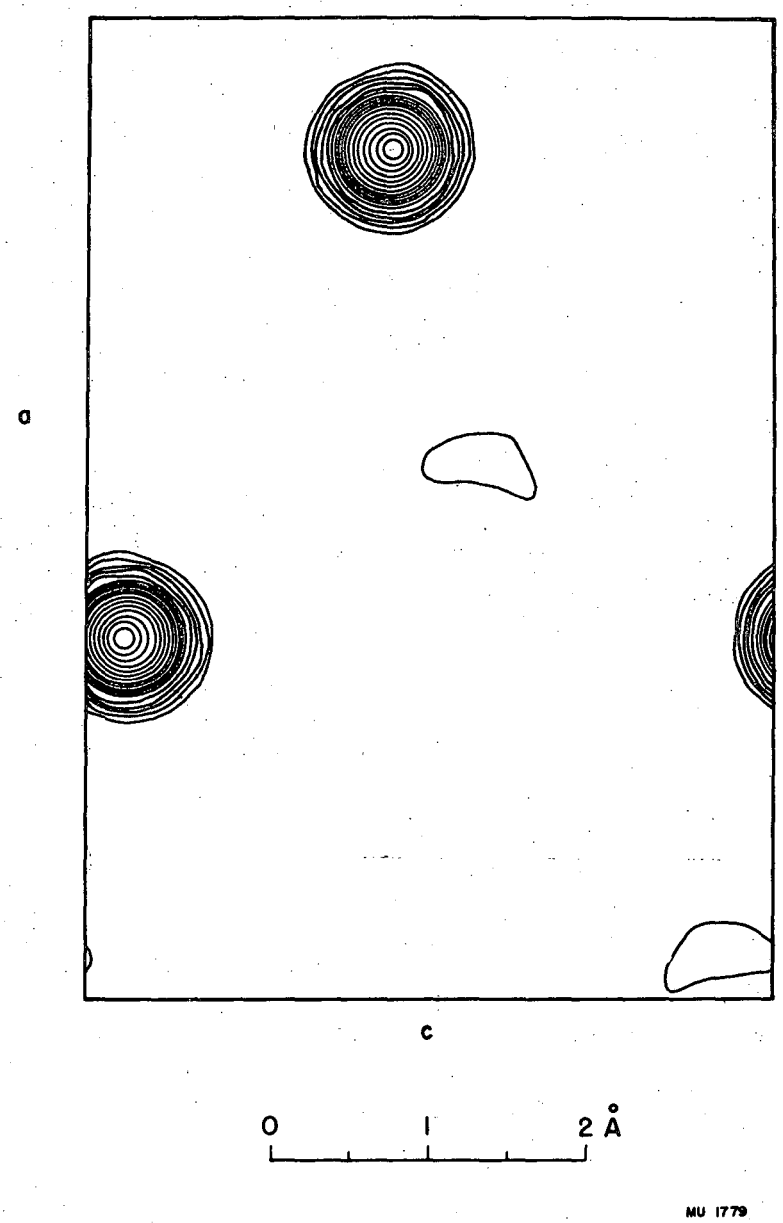

Fig. 14

The electron density section (040) plane for YF_3. Contours are in arbitrary units beginning at +100 and increasing in intervals of 100. 190 independent non-zero intensities were utilized. (F_{0k0} terms were omitted)

With these observations as aids in giving us a general idea of the fluoride ion location we proceeded to refine the fluoride ion parameters in such a way as to give us the most reasonable interionic distances. In all of the ensuing calculations the yttriums are considered fixed by the (040) section (Figure 14) at x = 0.366 and z = 0.059. A slight refinement will be made later, however.

Table 2 is now presented as a summary of all of the observed and calculated parameters for all of the ions. The four fold yttriums and fluorides are contained in set 4(c) and the eight fold fluorides in set 8(d). These positions will be given in greater detail shortly.

Table 2

		4 Y in 4(c)			4 F in 4(c)			8 F in 8(d)		
No. of Terms	Method of Calculation	x	y	z	x'	y'	z'	x''	y''	z''
19	a projection		0.250	0.057					0.09	0.34
26	c projection	0.366	0.250		0.55	0.250		0.17	0.04	
29	b projection	0.368		0.053				0.16		0.35
190	040 section	0.366		0.059	0.54		0.59			
	geometrically				0.528	0.250	0.601	0.165	0.060	0.363
	corrected values	0.367		0.058						

The last item, under corrected values, will be discussed more fully later. However, as mentioned above, all of the calculations forthcoming were ~~calculated~~ made with x = 0.366 and z = 0.059; the slight differences in the two values were not significant enough to warrant recalculating all of the values mentioned in this paper.

F. Description of Structure and Structure Amplitude Agreement

The interionic distances calculated using the geometrically established parameters for the fluoride ions are given in Table 3.

Table 3

Number of Distances	Nature of the Distance	Distance in Angstroms
1	4Y - 4F	2.26
1	4F	2.26
1	4F	2.59
2	4Y - 8F	2.26
2	8F	2.30
2	8F	2.33
1	4F - 4Y	2.26
1	4Y	2.26
1	4Y	2.59
2	4F - 8F	2.57
2	8F	2.71
2	8F	2.83
2	8F	2.85
1	8F - 4Y	2.26
1	4Y	2.30
1	4Y	2.33
1	8F - 4F	2.57
1	4F	2.71
1	4F	2.83
1	4F	2.85
1	8F - 8F	2.55
1	8F	2.58
1	8F	2.60

There are three sets of values in the previous table, one set for each kind of atom; the four fold yttriums, 4Y; the four fold fluorides, 4F; and the eight fold fluorides, 8F. The yttrium ion is surrounded by eight close neighbors, all fluoride ions, plus one distant one. The four fold fluoride ion has as closest neighbors two yttrium ions and two eight fold fluoride ions, with farther neighbors of six eight fold fluorides and one yttrium. The eight fold fluorides have three nearest yttrium neighbors, four nearest fluoride neighbors, and four further distant neighbors of fluorides.

Figure 15 was drawn to show the projection of the ions on the b face. The fluoride ions are represented by large circles and the yttrium ions by small circles; they are not to scale. Figure 16 was drawn as a packing drawing from Figure 15, still in the b projection. The large spheres represent fluoride ions, and the small spheres represent yttrium ions. They are drawn to scale with fluoride ion radius taken as 1.35 A and yttrium ion radius taken as 0.93 A.

The F values were then calculated and compared with the observed F values as is shown in Table 4. Table 4 gives the $hk\ell$, $\sin^2\theta$ as calculated on the basis of copper $K\alpha$ x-rays (λ = 1.5418 A), F calculated, F observed and improved, and F observed. The F observed values were those used in preparing the (040) density section, and were an average of all of the observed spots from all of the films.

The F observed and improved group are those obtained afterwards which give a slightly better agreement with the calculated; the improvement was made by readjusting some of the normalizing factors between various films obtained from different crystals to form a uniform set of values. Since the absorption factor was an unknown, it was not surprising to find the agreement varying between the various films.

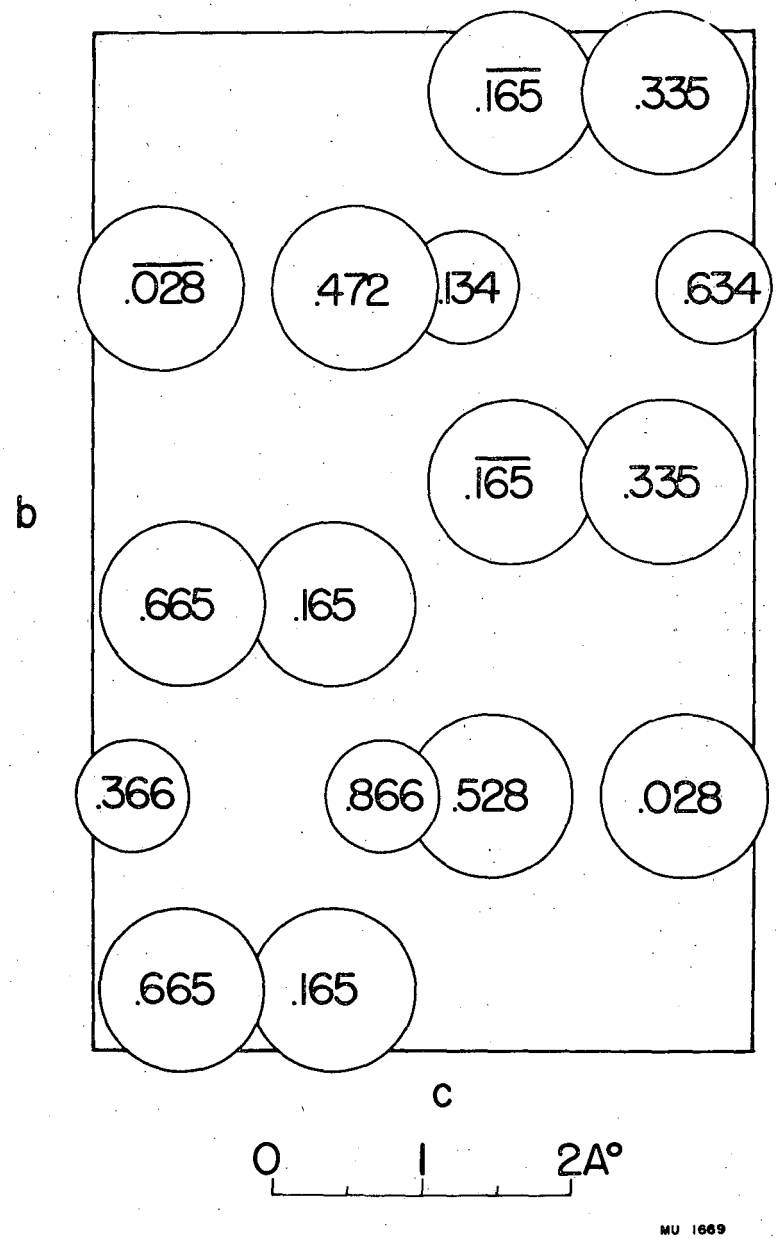

Fig. 15

A projection of the atomic contents of the orthorhombic unit of YF_3 on its a face. Large circles represent the fluorides.

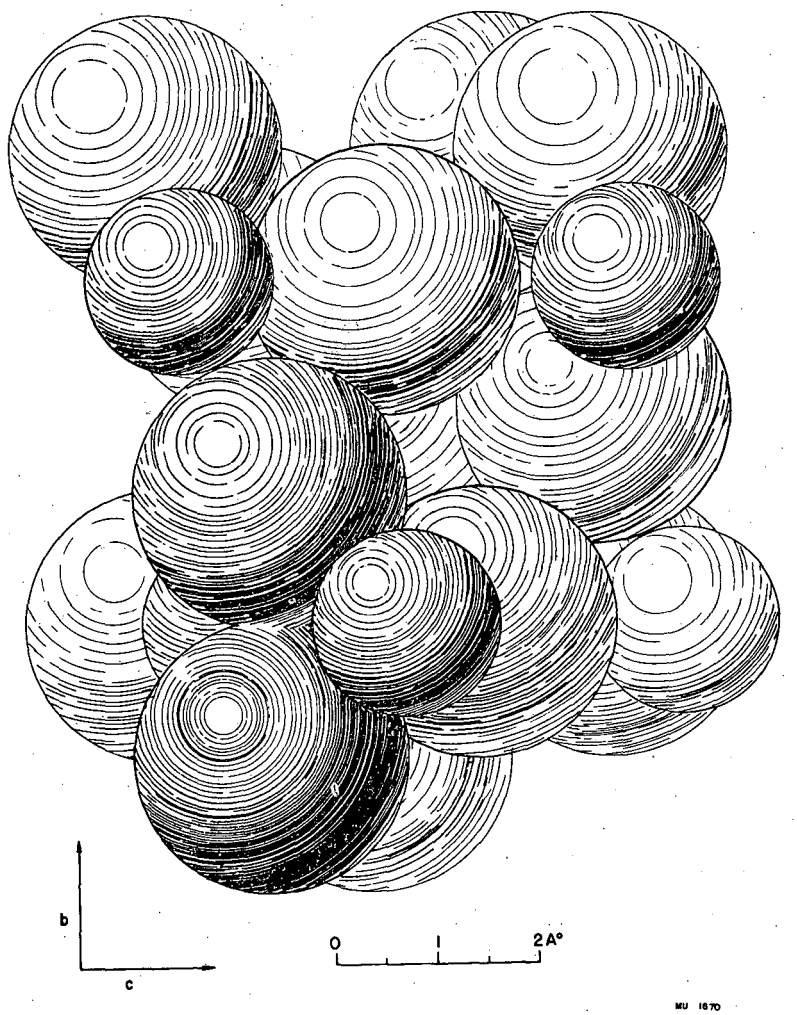

Fig. 16

A packing drawing of the structure of YF_3. Y and F are drawn with radii 1.35 A and 0.93 A, respectively.

The calculated F values were then used to recalculate the electron density in the vicinity of the yttrium peak to establish some correction for the fact that we have made a small error in taking a finite summation. When we used the calculated F values of Table 4 obtained from x = 0.366, and z = 0.059, the peak shifted to 0.365 and 0.060, respectively; therefore the corrected value for x and z was finally established at 0.367 and 0.058.

The value of the deviation was found from:

$$\frac{\Sigma \left| \left| F_{calc} \right| - \left| F_{obs} \right| \right|}{\Sigma \left| F_{obs} \right|} = 0.21 \qquad (7)$$

for the improved set and 0.23 for the original set. The final parameters are as follows:

Y 4(c) $x,1/4,z;\ \bar{x},3/4,\bar{z};\ 1/2-x,3/4,1/2+z;\ 1/2+x,1/4,1/2-z;$

$x = 0.367 \quad z = 0.058$

F 4(c) $x',1/4,z';\ \bar{x}',3/4,\bar{z}';\ 1/2-x',3/4,1/2+z';\ 1/2+x',1/4,1/2-z';$

$x' = 0.528 \quad z' = 0.601$

F 8(d) $x'',y'',z'';\ 1/2+x'',1/2-y'',1/2-z'';\ \bar{x}'',1/2+y'',\bar{z}'';\ 1/2-x'',\bar{y}'',\ 1/2+z'';$

$\bar{x}'',\bar{y}'',\bar{z}'';\ 1/2-x'',1/2+y'',1/2+z'';\ x'',1/2-y'',z'';\ 1/2+x'',y'',1/2-z'';$

$x'' = 0.165 \quad y'' = 0.060 \quad z'' = 0.363$

The estimated error in these parameters for Y are $\pm$ 0.001 and for the fluorides $\pm$ 0.002.

The YF_3 powder pattern was obtained and indexed with chromium Kα x-rays (2.2909 A) and the following lattice constants obtained:

a = 6.353 ± 0.003 A

b = 6.850 ± 0.003 A a:b:c = 0.9274: 1: 0.6413

c = 4.393 ± 0.003 A

Volume of one unit cell = 191.17 A^3

Molecular weight = 145.92

Calculated density = 5.069 g/cc

This structure seems to be in agreement with a few other isolated facts from the literature. Vogt (1914) reported that a melt of pure yttrium trifluoride gave biaxial plates, optically neutral with 2V ≅ 90°.

Nowacki (1938) reported the density of yttrium trifluoride, precipitated with hydrofluoric acid, as 5.15 g/cc as compared with our calculated value of 5.07 g/cc.

Table 4

hkℓ	$\sin^2\theta$	F Calculated	F Observed Improved	F Observed
000	0.0000	+234		
010	0.0127	0		
100	0.0148	0		
110	0.0275	0		
001	0.0308	0		
011	0.0435	-40	~~36~~ 34	35
101	0.0456	-67	~~41~~ 37	36
020	0.0507	-99	~~45~~ 50	41
111	0.0583	-69	41	51
200	0.0593	-13	10	8
120	0.0655	0		
210	0.0720	+81	~~45~~ 47	36
021	0.0815	0		
201	0.0901	+11	~~16~~ 17	15
121	0.0963	+34	~~33~~ 34	33
211	0.1028	+29	20	22
220	0.1100	-25	~~23~~ 26	21
030	0.1140	0		
002	0.1232	+71	~~55~~ 58	55

Table 4 (Cont.)

hkℓ	$\sin^2\theta$	F Calculated	F Observed Improved	F Observed
130	0.1288	0		
300	0.1333	0		
012	0.1359	0		
102	0.1380	-9	15	12
221	0.1408	-58	~~58~~ 48	49
031	0.1448	-6		
310	0.1460	0		
112	0.1507	+76	~~53~~ 50	51
131	0.1596	+86	~~75~~ 53	75
301	0.1641	+107	~~62~~ 53	52
230	0.1733	-112	~~60~~ 71	60
022	0.1739	-76	~~59~~ 57	50
311	0.1768	-55	~~49~~ 48	53
202	0.1825	0		
320	0.1840	0		
122	0.1887	+63	~~60~~ 51	49
212	0.1952	+64	~~54~~ 57	50
040	0.2026	+106	~~66~~ 72	60
231	0.2041	-1		
321	0.2148	-62	~~60~~ 49	53
140	0.2174	0		
222	0.2332	+4		
041	0.2334	0		
400	0.2371	-86	~~62~~ 69	60
032	0.2372	0		
330	0.2473	0		
141	0.2482	-39	~~45~~ 40	45
410	0.2498	-19	~~11~~ 13	10
132	0.2520	-38	~~47~~ 37	40
302	0.2565	-24	30	31
240	0.2619	+4		
401	0.2679	+18	~~13~~ 14	15
312	0.2692	-54	~~51~~ 46	47
003	0.2771	0		
331	0.2781	+48	~~58~~ 48	58
411	0.2806	+44	43	47
420	0.2878	+56	~~60~~ 63	54
013	0.2898	-69	~~60~~ 65	58
103	0.2920	-16	~~19~~ 18	19
241	0.2927	+30	~~26~~ 32	26
232	0.2965	-52	~~53~~ 55	53
113	0.3047	-32	~~32~~ 33	36
322	0.3072	+25	~~31~~ 32	33
050	0.3166	0		
421	0.3186	+13	~~15~~ 13	15

Table 4 (Cont.)

hkℓ	$\sin^2\theta$	F Calculated	F Observed Improved	F Observed
042	0.3258	+59	~~58~~ 61	58
023	0.3278	0		
150	0.3314	0		
340	0.3359	0		
203	0.3364	+60	~~66~~ 56	47
142	0.3406	-34	~~44~~ 39	40
123	0.3427	+34	~~37~~ 34	35
051	0.3474	-36	~~39~~ 41	45
213	0.3491	+22	~~17~~ 20	20
430	0.3511	+47	~~36~~ 47	36
402	0.3603	-48	53	52
151	0.3622	-40	~~49~~ 44	52
341	0.3667	+66	~~65~~ 52	65
500	0.3704	0		
332	0.3705	+14	~~15~~ 14	15
412	0.3730	-15	~~11~~ 14	13
250	0.3759	+49	~~56~~ 63	56
431	0.3819	-22	~~28~~ 23	28
510	0.3831	0		
242	0.3851	-3		
223	0.3871	-76	~~63~~ 72	71
033	0.3911	+46	~~42~~ 48	42
501	0.4012	+32	~~37~~ 38	40
133	0.4060	+8	~~12~~ 11	12
251	0.4067	+20	~~18~~ 17	18
303	0.4105	+3	~~10~~ 12	16
422	0.4110	+50	~~50~~ 51	50
511	0.4139	+46	~~46~~ 48	49
520	0.4211	0		
313	0.4232	-18	~~17~~ 20	22
440	0.4397	-61	~~55~~ 72	55
052	0.4398	0		
350	0.4499	0		
233	0.4504	-12	~~11~~ 12	11
521	0.4519	-42	~~41~~ 42	39
152	0.4546	+51	~~55~~ 52	56
060	0.4559	-93	~~70~~ 86	71
342	0.4591	-22	~~30~~ 23	30
323	0.4612	-35	~~32~~ 33	43
441	0.4705	-1		
160	0.4707	0		
432	0.4743	+11	~~13~~ 12	13
043	0.4798	0		
351	0.4807	-41	~~56~~ 47	56
530	0.4844	0		

Table 4 (Cont.)

hkℓ	$\sin^2\theta$	F Calculated	F Observed Improved	F Observed
061	0.4867	0		
004	0.4927	-22	~~21~~ 22	21
502	0.4936	+30	~~28~~ 31	32
143	0.4946	-23	~~25~~ 22	25
252	0.4991	+52	~~57~~ 53	57
161	0.5015	+39	~~47~~ 44	51
014	0.5045	0		
512	0.5063	-9	~~17~~ 20	20
104	0.5075	-54	~~49~~ 48	50
403	0.5142	+2		
260	0.5152	+1		
531	0.5152	-59	~~58~~ 53	58
114	0.5202	+48	~~49~~ 55	45
333	0.5245	+11	~~25~~ 17	25
413	0.5269	+74	~~59~~ 66	59
600	0.5334	+48	~~42~~ 40	36
243	0.5390	+62	~~67~~ 64	67
024	0.5434	-12		
522	0.5443	-60	~~56~~ 50	52
261	0.5460	-18	~~21~~ 18	21
610	0.5461	-71	~~65~~ 72	60
204	0.5520	+1		
450	0.5537	-5		
124	0.5582	+44	~~46~~ 44	46
442	0.5629	-45	~~47~~ 44	47
601	0.5642	-16	~~17~~ 18	20
214	0.5647	+15	~~11~~ 12	11
423	0.5649	+14		
540	0.5730	0		
352	0.5731	-46	~~59~~ 47	59
611	0.5769	-16	~~7~~ 8	7
062	0.5791	-49	55	54
620	0.5841	-12	~~10~~ 13	10
451	0.5845	+35	~~38~~ 37	38
360	0.5892	0		
053	0.5938	-59	~~56~~ 62	56
162	0.5939	+21	~~24~~ 21	24
224	0.6027	+14		
541	0.6038	+33	~~41~~ 36	41
034	0.6067	0		
532	0.6076	+22	~~27~~ 21	27
153	0.6068	-33	~~33~~ 30	33
343	0.6131	+20	~~35~~ 22	35
621	0.6149	+18	18	20
361	0.6200	-63	~~78~~ -58	78

Table 4 (Cont.)

hkℓ	$\sin^2\theta$	F Calculated	F Observed Improved	F Observed
070	0.6206	0		
134	0.6215	-50	~~49~~ 44	49
304	0.6260	-32	~~33~~ 34	46
433*	0.6282	-57		
170	0.6354	0		
262	0.6384	+2		
314	0.6387	-43	~~57~~ 47	57
630	0.6474	+78	~~58~~ 76	58
503	0.6476	+18	17	17
071	0.6514	+11	~~16~~ 17	16
253	0.6530	+19	~~21~~ 19	21
602	0.6566	+14	~~11~~ 14	16
513	0.6603	+32	~~27~~ 30	27
234	0.6660	+6		
171	0.6662	+49	~~58~~ 54	58
612	0.6693	-46	~~48~~ 46	47
324	0.6767	+31	~~36~~ 27	48
452	0.6769	-14	~~9~~ 8	9
631	0.6782	-7	~~6~~ 8	6
270	0.6799	-63	~~73~~ 79	73
550	0.6870	0		
460	0.6930	+60	~~57~~ 74	57
044	0.6953	-3		
542	0.6962	+43	~~40~~ 36	40
523	0.6983	-7		
622	0.7073	-18	~~13~~ 11	13
144	0.7101	-44	~~54~~ 48	54
271	0.7107	-4		
362	0.7124	+19	~~33~~ 16	33
443*	0.7168	-7		
551	0.7178	+34	~~41~~ 46	41
461	0.7238	-5		
700	0.7260	0		
353	0.7271	-18	~~27~~ 17	27
404	0.7298	-2		
063	0.7331	0		
640	0.7360	+25	~~25~~ 32	25
710	0.7387	0		
334	0.7400	+48	~~70~~ 47	70
414	0.7425	-2		
072	0.7438	0		
163	0.7479	+16	~~17~~ 16	17
370	0.7539	0		
244	0.7546	-7		
701	0.7568	-56	~~58~~ 55	61

Table 4 (Cont.)

hkℓ	$\sin^2\theta$	F Calculated	F Observed Improved	F Observed
172	0.7586	-30	~~36~~ 33	38
533*	0.7616	-14		
641	0.7668	-16	~~29~~ 24	29
711	0.7695	+18	~~22~~ 24	23
005	0.7699	0		
632	0.7706	+43	~~49~~ 44	49
720	0.7767	0		
424	0.7805	+16		
015	0.7825	-46	~~49~~ 52	47
105	0.7847	-3	9	9
371	0.7847	+35	~~40~~ 46	60
263	0.7923	-50	~~55~~ 53	55
115	0.7970	+12		
272	0.8031	-41	~~54~~ 48	54
721	0.8075	+45	~~39~~ 41	39
054	0.8093	0		
552	0.8102	-8	~~11~~ 10	11
603	0.8105	-43	47	47
080	0.8106	+51	~~52~~ 67	55
462	0.8162	+40	~~49~~ 43	49
025	0.8205	0		
613	0.8232	-20	~~9~~ 10	9
154	0.8241	+41	~~47~~ 43	47
180	0.8254	0		
560	0.8263	0		
344	0.8286	-31	~~63~~ 38	63
205	0.8291	+68	~~57~~ 54	54
453*	0.8308	+60		
125	0.8338	+2		
730	0.8400	0		
081	0.8414	0		
215	0.8418	0		
434*	0.8438	-14		
702	0.8492	+34	~~40~~ 36	39
650	0.8500	-59	~~55~~ 71	55
543*	0.8502	+11		
181	0.8562	-26	~~38~~ 35	41
561	0.8571	-27	~~45~~ 37	45
470	0.8577	+24	~~20~~ 26	20
642	0.8592	+15	~~19~~ 16	19
623	0.8612	+43	~~41~~ 42	41
712	0.8619	+44	39	39
504	0.8631	+58	53	53
363	0.8664	-11	~~27~~ 16	27
254	0.8686	+19	~~25~~ 23	25

Table 4 (Cont.)

hkℓ	$\sin^2\theta$	F Calculated	F Observed Improved	F Observed
280	0.8699	+8	~~6~~ 8	6
731	0.8708	-8	~~11~~ 14	11
514	0.8758	-26	~~27~~ 30	27
372	0.8771	+18	~~37~~ 28	37
225	0.8798	-46	~~50~~ 47	51
651	0.8808	-15	~~10~~ 12	10
035	0.8838	+67	~~51~~ 57	51
471	0.8885	-21	~~22~~ 28	22
135	0.8951	-18	~~14~~ 18	14
073	0.8977	+41	~~42~~ 48	43
722	0.8999	+17	~~18~~ 16	18
281	0.9007	+31	~~42~~ 36	42
305	0.9032	-25	27	38
173	0.9126	+13	~~17~~ 15	17
524	0.9138	-49	~~52~~ 48	52
315	0.9159	+13	~~10~~ 13	17
633	0.9245	+7		
740	0.9286	0		
444*	0.9324	-9		
082	0.9338	+46	~~41~~ 47	49
354	0.9426	-38	~~62~~ 44	62
235	0.9431	-11	11	11
380	0.9439	0		
800	0.9482	+46	~~50~~ 52	46
064	0.9486	+9		
182	0.9486	-39	~~46~~ 42	48
562	0.9495	-30	~~39~~ 35	39
325	0.9539	+15	~~18~~ 11	18
273	0.9570	-10	13	13
741	0.9594	-47	~~51~~ 41	51
810	0.9609	+13	11	10
732	0.9632	-32	~~33~~ 30	33
164	0.9634	+43	~~41~~ 38	41
553*	0.9642	+33		
463*	0.9701	+3		
045	0.9725	0		
652	0.9732	-40	~~47~~ 44	47
381	0.9747	+38	~~48~~ 35	48
534*	0.9771	+22		
801	0.9790	+4		
145	0.9809	+4		
472	0.9809	+10	~~9~~ 7	9
660+	0.9893	-30		
570+	0.9910	0		
811+	0.9917	-11		
282+	0.9931	-4		
820+	0.9989	-54	—	

*Not present on the set of films observed; all hkℓ whose values are 433 and above were not photographed here.

+$\sin^2\theta$ too large; spots are off films.

II. THE RARE EARTH FLUORIDES

A. Introduction

It was then decided to investigate all of the rare earth trifluorides, particularly those suspected to exhibit the orthorhombic (YF_3 type) structure. Two methods for preparing these compounds were used, a dry and a wet preparation. The two methods will be described in detail, and any deviations from these methods will be mentioned under the individual compounds later.

B. Experimental (Preparation)

The dry synthesis of YF_3, SmF_3, EuF_3, GdF_3, TmF_3 and YbF_3 was performed by others who were interested in these compounds for other purposes and submitted to us for x-ray analysis. These trifluorides were prepared in the following manner. Several milligrams of the sesquioxide were placed in a platinum crucible and then placed inside a platinum line apparatus. The platinum line was evacuated and a dry mixture of hydrogen and hydrogen fluoride gases were passed through the system. The temperature was raised and maintained at about 700°C for two hours; the line was cooled and evacuated. Powder patterns of the resulting material were obtained using chromium K alpha x-rays (λ = 2.909A). The hydrogen gas was probably not necessary except in the cases where oxidation to a higher state was possible, but it was apparently used anyway as part of the general procedure.

In order to complete the list of rare earth trifluorides as well as to obtain better diffracting samples, the following compounds, SmF_3, EuF_3, GdF_3, TbF_3, HoF_3, ErF_3, TmF_3, and LuF_3, were prepared by a wet precipitation as follows. From five to fifteen milligrams of the rare

earth oxide were dissolved in about four cubic centimeters of 6 N HCl. The solution was neutralized with 6 N NH_4OH until the gelatinous hydroxide appeared, and 6 N HCl (a few drops) was added until the hydroxide disappeared again. The resulting solution was transferred to a plastic, HF resistant, test tube and placed in a bath of hot water, 100°C. One to two cubic centimeters of concentrated hydrofluoric acid was added and the formation of a gelatinous precipitate was observed which coagulated and settled to the bottom as a fine white powder in a few minutes; the material was left in the bath for one hour. The precipitate was centrifuged, washed with water, and dried in an open oven between 100 and 150°C. The dried material was loaded into a platinum crucible and heated in an electric furnace in vacuum (10^{-5} to 10^{-6} mm of mercury) to a temperature between 1000 and 1400°C for one hour. The resulting material when photographed with x-rays, generally chromium K alpha x-rays (λ = 2.909 A), gave good sharp powder patterns which ~~lended themselves~~ suitable for accurate measurement of the cell constants. We reasoned later that perhaps it was not necessary to neutralize the dissolved rare earths before precipitation with the hydrofluoric acid. We did prepare EuF_3 and TmF_3 ~~by not~~ without neutralizing with ammonium hydroxide and did get slightly different results in the patterns of the unheated material. There was a tendency for the ammonium ion to form salts with the other ions in solution; these salts fortunately volatilized off the ammonia to yield the trifluorides on heating.

C. Experimental (Observations)

The preparation of each trifluoride and their powder patterns will be qualitatively discussed briefly. The quantitative data will follow later in chart form.

1. Yttrium Trifluoride.-- This compound was prepared by the dry method and has been well discussed previously.

2. Samarium Trifluoride.-- This compound has been reported previously as crystallizing in the hexagonal (LaF_3 type) form (Oftedal 1929).

This material was prepared by the dry method several times and resulted in one time being just the orthorhombic (YF_3 type) form and in another time just the hexagonal (LaF_3 type) form.

The material was also prepared by the wet method and the resulting dried powder, before being subjected to the heat treatment, gave good hexagonal patterns. However, after heating the material to 1000 to 1100°C, both orthorhombic and hexagonal phases were present simultaneously. Heating did not seem to affect the cell constants of the hexagonal phase.

A very pure samarium sesquioxide was used throughout. The material was provided by Speddings group at Iowa State College, purified by ion exchange resins, as were many of the rare earths used in this research.

3. Europium Trifluoride.-- A pure sample of Eu_2O_3 with no detectable (spectrographically) amounts of any other rare earths was used. The fluoride here was prepared by the dry method. The resulting powder patterns showed the orthorhombic form.

Nowacki (1938) reported that with 99.9% europium, he obtained EuF_3 which showed the ~~tysonite~~ hexagonal (LaF_3 type) structure, but he did not give any measurements on it. So we ~~did~~ made a second preparation of EuF_3, this time by the wet method. The material was prepared without the use of ammonium ion and the resulting dried material was found to exhibit the hexagonal structure. The material was not heated. Powder photographs were obtained on this hexagonal phase with the use of copper K alpha x-rays, (λ = 1.5418 A).

4. Gadolinium Trifluoride.-- This compound was prepared by the dry method. All of the measured lines were indexed on an orthorhombic (YF_3 type) cell. The Gd_2O_3 that was used as a beginning material was spectroscopically free of all rare earths except for a trace of ytterbium.

A wet precipitation was also ~~done~~ made and the resulting material photographed as the orthorhombic form.

5. Terbium Trifluoride.-- This compound was prepared by the wet method with a few minor variations. Six milligrams of brown Tb_4O_7, pure but for spectrographic traces of gadolinium, ytterbium, and calcium, was dissolved in about one cubic centimeter of 6 N HCl; the smaller amount of acid was used because this compound dissolved readily liberating ~~hydrogen~~ oxygen as it was ~~oxidized~~ reduced to the +3 terbium.

The dried unheated material showed the orthorhombic pattern when photographed, but the picture was of poor quality. After being heated to 1100°C for one hour, the material yielded excellent patterns of the orthorhombic form.

6. Dysprosium Trifluoride.-- The Dy_2O_3 used had 0.3% holmium and 0.35% ~~dysprosium~~ terbium and no other rare earths. This compound was prepared by the wet method. The dried unheated material gave diffuse patterns of the orthorhombic phase. After heating for one hour at 1400°C, the resulting photographs were greatly improved. No ~~real~~ evidence was present of a hexagonal phase.

Some of the DyF_3 was heated in air at about 500°C for ten hours, and it was converted entirely back to the oxide.

7. Holmium Trifluoride.-- Ho_2O_3, 99.8% pure with 0.2% impurities of other rare earths, was used. A departure from the established procedure in the wet method was attempted here. Instead of neutralizing with

ammonium hydroxide, sodium hydroxide was used. The material, on being heated to 1300°C, was completely volatilized; it was noticed that between 300 and 700°C there was a large increase in the pressure of the system which could not have been attributed to degassing of the crucibles.

The unheated material showed neither of the trifluoride type structures. There were two well crystallized phases present; one was a face centered cubic phase, and the other was a hexagonal phase; the possible interpretation of these two phases will be discussed later.

HoF_3 was then prepared properly following the original procedure outlined earlier. The unheated dried precipitate showed no trifluoride structure whatsoever, but did show a primitive cubic phase which was probably a mixed ammonium rare earth fluoride. This identical pattern showed up with erbium and thulium. This salt apparently volatilized the ammonia out completely with the heating as its pattern disappeared leaving behind the trifluoride structure. The material was heated 3/4 hours at 1100°C.

Two specimens were photographed: the first was a powder photograph of a solid chunk which resulted in a powder pattern which consisted primarily of a hexagonal (LaF_3 type) phase, with a much weaker orthorhombic (YF_3 type) phase; the second powder photograph was taken after the material was crushed and the resulting photograph showed the two phases present in about equal ~~intensity~~ amounts.

8. <u>Erbium Trifluoride</u>.-- Pink Er_2O_3, 99.9% pure with 0.1% other rare earths, was treated by the wet method. The dried unheated material gave the same cubic phase that the holmium did prior to being heated; there were no lines that could be attributed to any trifluoride type structure. After heating at 1300°C for an hour, a good powder pattern of the

orthorhombic form was obtained from the material.

9. Thulium Trifluoride.-- White Tm_2O_3 (spectrographically pure of lutetium, erbium, holmium, and yttrium but with <0.05% ytterbium impurity) was used. The material prepared by the dry method gave us fair orthorhombic patterns, but not good enough for accurate measurements at the big angles. The material was then prepared using the wet method. The dried unheated sample gave no trifluoride but just a cubic phase already observed in erbium and thulium. The heated (1000 to 1100°C for one hour) sample gave a mixed pattern of both trifluoride types (hexagonal and orthorhombic) in about equal intensities.

Another preparation of TmF_3 was undertaken with the purpose in mind of finding out the result of not neutralizing the original solution with ammonium hydroxide. The resulting dried precipitate gave the orthorhombic pattern when photographed with copper K alpha x-rays. The material was not heated, and the photographs were not measured.

10. Ytterbium Trifluoride.-- A sample of Yb_2O_3, containing spectrographic traces of calcium, copper, silver, and sodium but no rare earths, was used. The trifluoride was prepared by the dry method. The powder photographs gave the typical orthorhombic (YF_3 type) structure. No real evidence for a hexagonal phase was observed.

11. Lutetium Trifluoride.-- White Lu_2O_3 (with less than 0.2% thulium and ytterbium present) was used in the wet preparation. The unheated dried material gave numerous lines of apparently more than one compound, none of which could have been due to the trifluoride structures. After heating at 1000 to 1100°C for an hour, these phases disappeared leaving a material which gave photographs with chromium K alpha x-rays of the orthorhombic (YF_3 type) form.

12. General Observations.-- In many cases the final material gave extra lines which were not indexible. These were probably due to oxides, oxyfluorides, or other impurities.

In all cases the heated trifluorides were observed to be from gray to black in color. The unheated samples were always white. Even the yttrium trifluoride powder had a gray tinge to it. This observation has been made by others and remains unexplained so far.

D. Data on the Orthorhombic Trifluoride Structures

Table 5 summarizes the quantitative data on all of the orthorhombic powder patterns observed. Given are the compound, the three axial lengths in angstroms, the axial ratios, the unit cell volume in cubic angstroms (four metal ions in each cell), the molecular weight, and the x-ray calculated density in grams per cubic centimeter. The estimated error for the values of a, b, and c is between 0.06% and 0.10%.

The powder data for the orthorhombic trifluoride structures are presented in the following tables, numbers 6 through 17. Table 6 gives the calculated intensities for the trifluoride powder patterns on the basis of the YF_3 structure. Given are two sets of intensities: corrected and uncorrected for polarization. The Laurent's polarization correction ~~is~~ are made with the following formula:

$$I \propto \frac{1+\cos^2 2\theta}{\sin^2\theta \cos\theta} \cdot p \cdot \left|F\right|^2 \qquad (8)$$

where I - intensity, θ = Bragg reflection angle, p = multiplicity, and F = calculated structure factor. The multiplicity factor was introduced into both sets of intensities. An absorption correction was not made.

The purpose of the table was to set up a standard of comparison for the observed intensities of the powder pattern data in tables 7 through 17.

Tables 7 through 17 give the powder pattern data on all of the orthorhombic trifluoride patterns measured. Lines not indexed were also presented. All of the intensities observed were estimated visually, with no standard of comparison other than neighboring lines. The scale of the intensities used in order from the most intense to the least intense is as follows: vs, s+, s, s-, m+, m, m-, w+, w, w-, vw, vvw where v = very, s = strong, m = medium, w = weak. All $\sin^2\theta$'s given in tables 7 through 17 were on the basis of chromium K alpha x-rays, λ = ~~2.909~~ 2.2909 A.

In the cases of holmium and thulium trifluoride, the orthorhombic and hexagonal ~~phases~~ lines were both present on the same film; the hexagonal lines were separated out and presented later separately.

Table 5

Orthorhombic (YF_3 type) Rare Earth Trifluorides

Compound	Cell Dimensions in A a	b	c	Axial Ratios a/b/c	Unit Cell Volume A^3	Molecular Weight	Calculated Density g/cc
YF_3	6.353	6.850	4.393	.9274/1/.6413	191.17	145.92	5.069
SmF_3	6.669	7.059	4.405	.9447/1/.6240	207.37	207.43	6.643
EuF_3	6.622	7.019	4.396	.9434/1/.6263	204.33	209.0	6.793
GdF_3	6.570	6.984	4.393	.9407/1/.6290	201.57	213.9	7.047
TbF_3	6.513	6.949	4.384	.9373/1/.6309	198.41	216.2	7.236
DyF_3	6.460	6.906	4.376	.9354/1/.6336	195.23	219.46	7.465
HoF_3	6.404	6.875	4.379	.9314/1/.6369	192.80	221.94	7.644
ErF_3	6.354	6.846	4.380	.9281/1/.6398	190.53	224.2	7.814
TmF_3	6.283	6.811	4.408	.9224/1/.6471	188.63	226.4	7.971
YbF_3	6.216	6.786	4.434	.9160/1/.6534	187.03	230.04	8.168
LuF_3	6.151	6.758	4.467	.9102/1/.6610	185.69	232.99	8.332

Table 6

The Calculated Intensities for Orthorhombic YF_3 Powder Patterns

hkℓ	$p\|F\|^2$	Intensity Corrected for Polarization	hkℓ	$p\|F\|^2$	Intensity Corrected for Polarization
011	11	23	103	2	<1
101	30	64	241	12	<1
020	33	62	232	36	13
111	65	100	113	14	5
200	<1	<1	322	8	3
210	44	53	421	3	1
201	<1	<1	042	24	9
121	16	14	203	24	10
211	11	8	142	16	7
220	4	3	123	16	7
002	17	11	051	9	4
102	<1	<1	213	7	3
221	46	24	430	15	7
112	78	39	402	16	7
131	100	46	151	22	10
301	77	35	341	59	28
230	84	36	332	3	1
022	39	17	412	3	1
311	41	17	250	16	8
122	54	21	431	14	7
212	55	21	223	78	43
040	38	14	033	14	8
321	51	18	501	7	4
400	25	8	251	5	4
141	20	7	422	34	24
410	3	<1	511	28	21
132	19	6	313	4	3
302	4	1	440	25	34
401	2	<1	233	1	
312	41	13	521	23	
331	31	10	152	35	
411	26	9	060	29	
420	22	7	342	7	
013	32	11	323	48	

*Chromium K alpha x-rays
(λ = ~~2.909~~ 2.2909 A)

Table 7

YF_3 Orthorhombic Powder Pattern

Observed Intensities	hkℓ	$\sin^2\theta$* Calculated	$\sin^2\theta$* Observed	Observed Intensities	hkℓ	$\sin^2\theta$* Calculated	$\sin^2\theta$* Observed
m	011	.0960	.0960	w	411	.6162	.6155
s-	101	.1005	.1006	w	420	.6320	.6324
s-	020	.1118	.1118	w+	013	.6401	.6400
vs	111	.1285	.1283	w	241	.6450	.6459
s-	210	.1580	.1581	m	232	.6535	.6529
m+	121	.2123	.2122	w	113	.6726	.6727
w	211	.2260	.2264	w	322	.6764	.6758
vw	220	.2418	.2423	m-	042	.7188	.7189
m-	002	.2720	.2716	w+	203	.7421	.7421
m-	221	.3098	.3103	w	142	.7515	.7517
s	112	.3325	.3324	w	123	.7564	.7560
s	131	.3520	.3523	w-	051	.7665	.7673
m+	301	.3606	.3608	w	402	.7922	.7922
m-	230	.3815	.3818	w+	151	.7990	.7994
m-	022	.3838	.3833	s-	341	.8076	.8074
m	311	.3886	.3887	vw	332	.8161	.8179
m	122	.4163	.4163	m	250	.8285	.8289
m	212	.4300	.4299	w	431	.8397	.8400
w+	040	.4470	.4470	s	223	.8539	.8537
m-	321	.4724	.4723	w	033	.8636	.8631
w	400	.5202	.5211	vw	501	.8808	.8808
w+	141	.5475	.5483	vw	251	.8865	.8923
w	132	.5560	.5557	m	422	.9049	.9043
vw	302	.5646	.5647	w	511	.9088	.9082
m-	312	.5926	.5927	vw	313	.9327	.9315
w+	331	.6121	.6121	s	440	.9672	.9674

*Chromium K alpha x-ray (λ = ~~2.909~~ 2.2909 A)
a = 6.353 A; b = 6.850 A; c = 4.393 A

Table 8

SmF_3 Orthorhombic Powder Pattern

Observed Intensities	hkℓ	$\sin^2\theta$* Calculated	Observed
w	011	.0939	.0944
m	101	.0971	.0966
m	020	.1053	.1060
s	111	.1234	.1233
s	210	.1443	.1444
w	121	.2024	.2025
w	002	.2705	.2699
m	221	.2909	.2909
m	112	.3263	.3272
s	301	.3332	.3339
	131	.3341	
m	230	.3550	.3550
w	311	.3594	.3597
w	022	.3757	.3768
m	122	.4053	.4065
w	212	.4149	.4158
w	040	.4212	.4213
m	321	.4384	.4387
w	400	.4720	.4730
w	141	.5184	.5183
w	132	.5371	.5371
vw	312	.5624	.5630
vw	331	.5709	.5706
m	232	.6258	.6260
w	013	.6351	.6351
w	042	.6917	.6925
vw	203	.7266	.7262
m	341	.7546	.7548
vw	123	.7434	.7429
w	250	.7770	.7768
m	511	.8315	.8315
	223	.8320	
w	422	.8479	.8470
w	440	.8933	.8930
w	521	.9104	.9100
m	060	.9479	.9478
w	152	.9584	.9582

*Chromium K alpha x-rays (λ = ~~2.909~~ 2.2909 A)
a = 6.669 A; b = 7.059 A; c = 4.405 A

Table 9

EuF_3 Orthorhombic Powder Pattern

Observed Intensities	hkℓ	$\sin^2\theta$* Calculated	$\sin^2\theta$* Observed
w	011	.0946	.0948
m+	101	.0978	.0976
m	020	.1065	.1066
s	111	.1244	.1243
s-	210	.1463	.1462
m-	121	.2043	.2043
m-	002	.2716	.2715
m	221	.2941	.2941
m	112	.3281	.3285
s	301	.3372	.3382
	131	.3375	
m+	230	.3594	.3600
m-	311	.3638	.3640
w+	022	.3781	.3784
m	122	.4080	.4084
m-	212	.4179	.4180
m-	040	.4261	.4264
m	321	.4437	.4446
m-	400	.4787	.4785
m-	141	.5239	.5244
w	132	.5412	.5410
m	312	.5675	.5682
w	411	.5732	.5767
	331	.5769	
m-	420	.5852	.5854
vw	241	.6137	.6144
m	232	.6310	.6309
m-	013	.6377	.6382
w-	322	.6474	.6482
w	042	.6976	.6973
w+	203	.7308	.7298
w	402	.7503	.7492
s-	341	.7633	.7637
m-	250	.7855	.7861
s	223	.8372	.8374
m-	422	.8568	.8575
m	440	.9048	.9045
m	521	.9224	.9225
m+	060	.9587	.9589
s-	152	.9673	.9671
Unindexed Lines			
w			.1038
vvw			.1366
w+			.2794
vvw			.3140
vw			.6052

*Chromium K alpha x-rays (λ = 2.2909 A)
a = 6.622 A; b = 7.019 A; c = 4.396 A

Table 10

GdF_3 Orthorhombic Powder Pattern

Observed Intensities	hkℓ	$\sin^2\theta$* Calculated	$\sin^2\theta$* Observed
m-	011	.0949	.0943
m	101	.0984	.0982
m	020	.1076	.1073
s	111	.1253	.1246
s	210	.1485	.1481
vw	201	.1896	.1897
m	121	.2060	.2060
vw	211	.2165	.2159
m	002	.2720	.2718
m	221	.2972	.2962
m	112	.3293	.3295
s	131	.3405	.3409
	301	.3416	
m	230	.3637	.3630
m-	311	.3685	.3684
m	022	.3796	.3796
m	122	.4100	.4092
m	212	.4205	.4201
m	040	.4304	.4311
s	321	.4492	.4486
m	400	.4864	.4860
m	141	.5288	.5279
m	132	.5445	.5445
m	312	.5725	.5713
m	411	.5813	.5824
	331	.5837	
m	420	.5940	.5942
w	241	.6200	.6196
s	232	.6357	.6372
	013	.6389	
w	322	.6532	.6525
vw	113	.6693	.6697
m	042	.7024	.7026
s	142	.7328	.7334
	203	.7336	
vw	051	.7405	.7406
vw	123	.7500	.7502
m	402	.7584	.7583
s	341	.7720	.7723
w	332	.7877	.7865
s	250	.7941	.7942
w	501	.8280	.8279
s+	223	.8412	.8418
s	033	.8541	.8544
	511	.8549	
s	422	.8660	.8663
s	440	.9168	.9171
s	521	.9356	.9358
s	060	.9684	.9683
s	152	.9749	.9751

*Chromium K alpha x-rays (λ = 2.2909 A)
a = 6.570; b = 6.984; c = 4.393

Table 11

TbF_3 Orthorhombic Powder Pattern

Observed Intensities	hkℓ	$\sin^2\theta$* Calculated	$\sin^2\theta$* Observed
m	011	.0955	.0951
s	101	.0992	.0987
s	020	.1087	.1075
s	111	.1264	.1260
m	210	.1510	.1509
vw	201	.1921	.1917
w	121	.2079	.2074
vw	211	.2193	.2187
vw	220	.2325	.2316
m	002	.2731	.2732
m	221	.3008	.3013
m	112	.3312	.3311
s	131	.3437	.3437
m	301	.3467	.3463
m	230	.3683	.3687
w	311	.3739	.3746
m	022	.3818	.3821
m	122	.4127	.4125
m+	212	.4241	.4245
m	040	.4347	.4351
m+	321	.4554	.4559
m	400	.4948	.4963
vw	410	.5220	.5225
m	141	.5339	.5347
m	132	.5485	.5490
m	312	.5787	.5793
m	411	.5902	.5913
	331	.5913	
m	420	.6035	.6050
w	241	.6268	.6276
s	013	.6416	.6420
	232	.6414	
w+	322	.6602	.6605
w+	113	.6725	.6725
m	042	.7078	.7080
m+	203	.7382	.7392
	430	.7393	
vw	051	.7475	.7479
vw	123	.7540	.7532
w+	402	.7679	.7679
w	151	.7784	.7786
s-	341	.7814	.7809
w	412	.7951	.7959
m	250	.8030	.8031
s	223	.8469	.8466
w	033	.8588	.8583
m	511	.8687	.8687
m	422	.8766	.8768
w	313	.9200	.9188
m	440	.9295	.9295
m	521	.9502	.9501
s	060	.9781	.9782
m	152	.9832	.9827
Unindexed Lines			
vw			.4653
vw			.5101

*Chromium K alpha x-ray (λ = ~~2.909~~ 2.2909 A)
a = 6.513; b = 6.949; c = 4.384

Table 12

DyF_3 Orthorhombic Powder Pattern

Observed Intensities	hkℓ	$\sin^2\theta$* Calculated	$\sin^2\theta$* Observed
m	011	.0960	.0958
s	101	.0999	.0997
s	020	.1100	.1085
s	111	.1274	.1260
m	210	.1533	.1520
vw	201	.1943	.1948
m	121	.2099	.2077
vw	211	.2218	.2214
m	002	.2740	.2739
m	221	.3043	.3051
m+	112	.3329	.3328
s	131	.3475	.3480
m	301	.3515	.3520
s-	230	.3734	.3736
m	311	.3790	.3792
m	022	.3840	.3841
m	122	.4154	.4151
m	212	.4273	.4275
m	040	.4402	.4406
m	321	.4615	.4616
m-	400	.5030	.5037
m	141	.5401	.5403
m-	132	.5530	.5526
m	312	.5845	.5839
m+	331	.5991	.6000
	411	.5990	
m	420	.6130	.6142
w	241	.6345	.6356
m	013	.6441	.6465
	232	.6476	
vw	322	.6670	.6681
vw	113	.6755	.6759
m	042	.7142	.7146
m	142	.7456	.7441
	203	.7424	
w	051	.7563	.7572
	123	.7580	
w	402	.7770	.7776
m-	151	.7877	.7874
m	341	.7917	.7919
w	332	.8041	.8051
	412	.8047	
s	250	.8136	.8132
s	223	.8524	.8528
w	033	.8642	.8637
m	511	.8820	.8823
w	422	.8872	.8873
vw	313	.9271	.9263
m	440	.9432	.9430
m	521	.9645	.9645
Unindexed Lines			
vw			.1171
vw			.1401

*Chromium K alpha x-ray (λ = ~~2.909~~ 2.2909 A)
a = 6.460; b = 6.906; c = 4.376

Table 13

HoF_3 Orthorhombic Powder Pattern

Observed Intensities	hkℓ	$\sin^2\theta$* Calculated	$\sin^2\theta$* Observed
w+	011	.0962	.0959
m	101	.1004	.1002
m+	020	.1111	.1111
s-	111	.1282	.1283
m	210	.1558	.1557
vw	201	.1964	.1966
m	121	.2115	.2112
w	211	.2242	.2259
w	002	.2737	.2738
m-	221	.3075	.3074
w	112	.3335	.3338
m	131	.3502	.3506
s	301	.3563	.3558
m	230	.3769	.3777
	022	.3815	
m	311	.3841	.3846
w	122	.4168	.4170
m+	321	.4674	.4677
w-	400	.5118	.5119
w+	141	.5445	.5445
w	132	.5555	.5561
m-	312	.5894	.5894
m-	331	.6061	.6071
	411	.6080	
w+	420	.6229	.6230
w	013	.6436	.6422
	241	.6405	
m-	232	.6515	.6517
w	113	.6756	.6741
	322	.6726	
s-	421	.6912	.6922
m-	042	.7178	.7179
w-	203	.7439	.7439
w-	142	.7498	.7497
w	430	.7641	.7651
s	402	.7855	.7852
m-	151	.7942	.7942
m	341	.8004	.8007
w	250	.8220	.8217
s	223	.8550	.8550
vw	501	.8681	.8672
s	422	.8966	.8965
	511	.8960	
w+	440	.9559	.9564
m-	521	.9792	.9790

*Chromium K alpha x-ray (λ = ~~2.909~~ 2.2909 A)

Table 14

ErF_3 Orthorhombic Powder Pattern

Observed Intensities	hkℓ	$\sin^2\theta$* Calculated	$\sin^2\theta$* Observed
m-	011	.0964	.0960
m+	101	.1008	.1008
s-	020	.1119	.1121
s	111	.1288	.1285
s	210	.1580	.1576
w-	201	.1984	.1981
m	121	.2127	.2124
vw	211	.2264	.2261
m-	002	.2735	.2736
w+	221	.3103	.3106
m	112	.3340	.3338
s-	131	.3527	.3532
m+	301	.3609	.3612
s-	230	.3819	.3819
w	311	.3889	.3884
m-	122	.4179	.4182
s-	212	.4316	.4320
m	040	.4479	.4484
m+	321	.4728	.4731
m	400	.5200	.5201
m	141	.5487	.5488
w	132	.5579	.5582
vw	302	.5661	.5653
m	312	.5941	.5935
m+	331	.6128	.6125
vw	411	.6163	.6154
w+	420	.6319	.6313
m	013	.6434	.6440
	241	.6463	.6463

Observed Intensities	hkℓ	$\sin^2\theta$* Calculated	$\sin^2\theta$* Observed
m+	232	.6555	.6556
m	113	.6759	.6769
	322	.6780	
m	042	.7211	.7215
m	203	.7454	.7450
w+	142	.7537	.7538
vw	123	.7599	.7607
w	430	.7719	.7713
	213	.7734	
w	402	.7935	.7933
m	151	.8006	.8005
s	341	.8088	.8095
vw	332	.8179	.8183
m	250	.8298	.8298
w	431	.8402	.8402
s	223	.8573	.8574
m-	033	.8673	.8674
w	501	.8809	.8810
s-	422	.9054	.9054
m	511	.9091	.9088
w-	313	.9359	.9363
s	440	.9679	.9678
Unindexed Lines			
w+			.1411
vw			.1716
w			.3438
vvw			.4841
vvw			.4925
vw			.6888

*Chromium K alpha x-rays (λ = ~~2.909~~ 2.2909 A)
a = 6.354; b = 6.846; c = 4.380

Table 15

TmF_3 Orthorhombic Powder Pattern

Observed Intensities	hkℓ	$\sin^2\theta$* Calculated	$\sin^2\theta$* Observed
m-	011	.0958	.0962
s	101	.1007	.1012
s	020	.1131	.1136
s+	111	.1290	.1293
m+	210	.1613	.1622
m	121	.2138	.2144
w	002	.2701	.2702
m	221	.3136	.3146
w	112	.3316	.3318
s	131	.3552	.3550
m	301	.3667	.3613
w	022	.3832	.3829
m	230	.3875	.3884
w	311	.3950	.3959
w	122	.4164	.4161
m	212	.4313	.4309
s	040	.4525	.4526
m	321	.4798	.4808
w	400	.5318	.5335
m	141	.5532	.5528
w	132	.5578	.5578
m	312	.5975	.5980
m	331	.6212	.6223
vw	411	.6276	.6292
w-	013	.6360	.6356
w+	420	.6449	.6464
s	232	.6575	.6580
vw	113	.6692	.6686
w	322	.6823	.6836
m	042	.7226	.7226
w	203	.7407	.7409
m	123	.7540	.7550
	142	.7558	
vw	051	.7745	.7738
w	402	.8019	.8015
w	151	.8077	.8077
m	341	.8192	.8198
m	250	.8400	.8399
s	223	.8538	.8538
	431	.8538	
vw	033	.8622	.8623
vw	501	.8985	.8971
s	422	.9150	.9153
m	511	.9268	.9270

*Chromium K alpha x-rays (λ = ~~2.909~~ 2.2907 A)
a = 6.283; b = 6.811; c = 4.408

Table 16

YbF_3 Orthorhombic Powder Pattern

Observed Intensities	hkℓ	$\sin^2\theta$* Calculated	$\sin^2\theta$* Observed
vw	011	.0953	.0959
m+	101	.1008	.1015
m	020	.1137	.1139
s	111	.1293	.1294
s-	210	.1644	.1641
m+	121	.2147	.2144
w	002	.2671	.2674
m-	221	.3165	.3166
m	112	.3294	.3290
s	131	.3572	.3575
m	301	.3724	.3730
m-	022	.3809	.3814
m+	230	.3923	.3928
m-	311	.4009	.4015
w+	122	.4149	.4156
m+	212	.4313	.4309
m-	040	.4558	.4557
m	321	.4860	.4866
w	400	.5435	.5431
m	132	.5575	.5568
w+	312	.6010	.6021
m+	331	.6286	.6296
	013	.6295	
vw	411	.6383	.6392
	420	.6569	
s	241	.6585	.6588
	232	.6592	
vvw	322	.6863	.6863
m-	042	.6228	.7231
	421	.7237	
m-	203	.7368	.7364
w	123	.7489	.7476
w	142	.7569	.7575
vw	051	.7790	.7790
vvw	430	.7994	.8012
w	402	.8101	.8103
m+	151	.8130	.8125
s	341	.8281	.8278
m	250	.8480	.8487
s	223	.8505	.8508
vvw	431	.8659	.8632
vvw	501	.9153	.9159
	251	.9148	
s	422	.9238	.9246
m	511	.9438	.9440

*Chromium K alpha x-rays (λ = ~~2.909~~ 2.2909 A)
a = 6.216; b = 6.786; c = 4.434

Table 17

LuF_3 Orthorhombic Powder Pattern

Observed Intensities	hkℓ	$\sin^2\theta$* Calculated	$\sin^2\theta$* Observed
w	011	.0945	.0946
m	101	.1005	.1009
m	020	.1149	.1158
s	111	.1293	.1298
m	210	.1675	.1685
vw	201	.2046	.2058
m	121	.2156	.2160
vw	211	.2332	.2352
w	002	.2630	.2637
m	221	.3174	.3193
m-	112	.3284	.3272
m+	131	.3591	.3597
s-	022	.3798	.3794
	301	.3779	
s-	230	.3973	.3988
w+	311	.4066	.4073
w+	122	.4146	.4130
m	212	.4304	.4308
m	040	.4597	.4606
m+	321	.4928	.4943
w	132	.5563	.5562
	400	.5549	
m	141	.5602	.5608
vw	302	.5751	.5756

Observed Intensities	hkℓ	$\sin^2\theta$* Calculated	$\sin^2\theta$* Observed
m-	312	.6038	.6047
vw	013	.6205	.6212
m	331	.6365	.6372
m	232	.6606	.6608
w	420	.6697	.6714
m-	042	.7227	.7226
vw	203	.7306	.7307
vw	123	.7414	.7414
w	142	.7574	.7573
vw	051	.7841	.7840
s	151	.8188	.8184
	402	.8178	
m+	341	.8376	.8378
m-	223	.8454	.8460
m	250	.8570	.8570
s-	422	.9328	.9326
m	511	.9615	.9615
Unindexed Lines			
w			.1230
w			.1350
vw			.3454
w			.4458
vw			.4765
vw			.6801
vw			.7712

* Chromium K alpha x-rays (λ = ~~2.909~~ 2.2909 A)
a = 6.151; b - 6.758; c = 4.467

E. The Hexagonal Rare Earth Trifluorides

The hexagonal SmF_3, EuF_3, HoF_3, and TmF_3 were observed and measured. LaF_3, CeF_3, PrF_3, NdF_3, and SmF_3; and AcF_3, UF_3, NpF_3, PuF_3, and AmF_3, have been reported by Oftedal (1929, 1931) and Zachariasen (1948), respectively, as having the hexagonal LaF_3 type structure. Nowacki (1938) also observed the hexagonal EuF_3 but never reported any measurements. Table 18 summarizes all of the hexagonal structures.

SmF_3 was measured by Oftedal (1929), but significantly different cell constants were obtained here and ~~were~~ will be reported. In light of the value obtained for EuF_3, the SmF_3 constants reported in this paper were found to be more in line with the first four trifluorides (lanthanum, cerium, palladium, and neodymium) reported by Oftedal (1929) than the constants for the SmF_3 already reported by Oftedal (1929).

Tables 18 through 21 contain the powder pattern data observed from the photographs of SmF_3, EuF_3, HoF_3 and TmF_3. The radiation used will be found in the respective tables.

The data for the holmium and thulium trifluorides were separated out from among their orthorhombic patterns.

All values from the literature have been corrected from kX units to angstroms.

Table 18

The Hexagonal (LaF_3 type) Lanthanide and Actinide Trifluorides

Atomic Number	Compound	Cell Constants A a	c	c/a	Unit Cell Volume A^3	X-ray Density g/cc	Reference
57	LaF_3	7.177	7.344	1.023	327.59	5.957	Oftedal 1929, 1931
	Tysonite $(La-Ce)F_3$	7.138	7.295	1.022	321.88		Oftedal 1929, 1931
58	CeF_3	7.128	7.288	1.022	320.67	6.124	Oftedal 1929, 1931
59	PrF_3	7.075	7.232	1.022	313.49	6.289	Oftedal 1929, 1931
60	NdF_3	7.035	7.210	1.025	309.01	6.488	Oftedal 1929, 1931
62	SmF_3	6.99	7.16	1.024	303.0	6.82	Oftedal 1929, 1931
62	SmF_3	6.956	7.120	1.024	298.34	6.925	Zalkin
63	EuF_3	6.916	7.091	1.025	293.72	7.088	Zalkin
67	HoF_3	6.833	6.984	1.022	282.40	7.829	Zalkin
69	TmF_3	6.763	6.927	1.024	274.37	8.220	Zalkin
89	AcF_3	7.41	7.55	1.023	359.0		Zachariasen 1948
92	UF_3	7.181	7.348	1.023	328.13	8.959	Zachariasen 1948
93	NpF_3	7.129	7.288	1.022	320.77		Zachariasen 1948
94	PuF_3	7.093	7.254	1.023	315.86		Zachariasen 1948
95	AmF_3	7.065	7.240	1.025	312.76		Zachariasen 1948

Table 19

SmF_3 Hexagonal Powder Pattern

Observed Intensities	hkℓ	$\sin^2\theta$* Calculated	$\sin^2\theta$* Observed
m	002	.1035	.1029
m	110	.1085	.1079
s	111	.1344	.1339
w-	112	.2120	.2118
s-	300	.3254	.3259
s-	113	.3414	.3415
vw	004	.4141	.4163
m+	302	.4290	.4292
m-	221	.4598	.4597
vw	114	.5226	.5222
vw	222	.5374	.5371
m	223	.6668	.6671
w+	304	.7395	.7393
w+	410	.7594	.7577
s-	411	.7852	.7855
w	224	.8480	.8472
w	412	.8629	.8625
w	006	.9317	.9317
m+	330	.9763	.9764

*Chromium K alpha x-rays (λ = ~~2.909~~ 2.2909 A)
a = 6.956; c = 7.120

Table 20

EuF_3 Hexagonal Powder Pattern

Observed Intensities	hkℓ	$\sin^2\theta$* Calculated	$\sin^2\theta$* Observed
m	002	.0473	.0477
s	111	.0615	.0617
m	112	.0969	.0968
s	300	.1490	.1487
s	113	.1560	.1559
w	004	.1891	.1888
m+	302	.1963	.1964
w	221	.2106	.2105
w	114	.2388	.2382
w	222	.2460	.2466
m	223	.3051	.3051
m	304	.3381	.3383
m-	410	.3478	.3464
	115	.3451	
m+	411	.3596	.3605
w	412	.3951	.3960
m	413	.4542	.4548
w	116	.4752	.4766
m	225	.4943	.4942
	332	.4944	
w+	414	.5369	.5351
m	306	.5745	.5751
w	600	.5965	.5954
vw	117	.6288	.6271
vw	226	.6243	.6255
m	415	.6433	.6438
	602	.6436	
m-	521	.6576	.6574
w	522	.6932	.6939
m	416	.7733	.7529
w	604	.7854	.7836
m	118	.8061	.8070
	441	.8071	
m	336	.8727	.8732
m	308	.9055	.9052
m	417	.9270	.9270
m	525	.9414	.9416
m	228	.9552	.9555
	711	.9559	
Unindexed Lines			
w			.0553
w			.0657
vw			.0835
w			.5212

*Copper K alpha x-rays (λ = 1.5418 A)
a = 6.916; c = 7.091

Table 21

HoF_3 Hexagonal Powder Pattern

Observed Intensities	hkℓ	$\sin^2\theta$* Calculated	Observed
m-	002	.1076	.1076
w	110	.1124	.1124
s+	111	.1393	.1392
w+	112	.2200	.2204
m	300	.3373	.3379
s	113	.3545	.3558
m	004	.4304	.4297
s	302	.4449	.4451
m+	221	.4766	.4770
w+	114	.5428	.5439
w	222	.5573	.5561
s	223	.6918	.6926
s	304	.7677	.7682
m	115	.7849	.7852
s	410	.7868	.7856
s	411	.8138	.8140
w	224	.8801	.8805
m	006	.9684	.9682

*Chromium K alpha x-rays (λ = ~~2.909~~ 2.2909 A)
a = 6.833; c = 6.984

Table 22

TmF_3 Hexagonal Powder Pattern

Observed Intensities	hkℓ	$\sin^2\theta$* Calculated	Observed
m	002	.1094	.1098
s	110	.1147	.1136
s-	111	.1420	.1423
w	112	.2241	.2246
m	300	.3441	.3443
s	113	.3608	.3613
w	004	.4374	.4380
s	302	.4535	.4526
w	221	.4861	.4857
m	114	.5521	.5528
w	222	.5682	.5679
w	223	.7049	.7051
m	304	.7815	.7812
w	115	.7982	.7974
m	411	.8302	.8299
vw	224	.8962	.8971
s	006	.9842	.9842

*Chromium K alpha x-rays (λ = ~~2.909~~ 2.2909 A)
a = 6.763; c = 6.927

F. Other Analogous RX_3 Structures

1. Fe_3C - Cementite.-- The crystal structure of this material was determined and measured (Lipson, Petch 1940)(Hume-Rothery, Rayner and Little 1942) as orthorhombic having had the same space group as we reported for yttrium trifluoride; the cell constants for Fe_3C were reported as a = 5.077 kX; b = 6.727 kX; c = 4.515 kX. Although the cementite structure had a similar packing as yttrium trifluoride, there were too many differences in the two compounds to consider them as being really iso-structural.

The axial ratios were considerably different:

$$YF_3 \quad a/b/c = .9724/1/.6413$$
$$Fe_3C \quad a/b/c = .7547/1/.6711$$

In the cementite structure the heavy positive iron atoms occupied positions corresponding to the light negative fluoride ions in the yttrium trifluoride structure. The trifluoride could have been considered at best a pseudo-anticementite structure.

The interatomic distances in cementite best agreed with metallic radio for the iron and the carbon; in yttrium trifluoride the distances best agreed with ionic radii for the yttrium and fluorine. Thus YF_3 as compared with Fe_3C was somewhat of a different type compound, ionic versus metallic type compound, respectively.

2. BiF_3 - Bismuth Trifluoride.-- An orthorhombic structure for BiF_3 has been reported by Zachariasen (1949[2]) having a = 6.56 A; b = 7.03 A; c = 4.86 A, a/b/c = .933/1/.691.

This compound was considered to be of the yttrium trifluoride type considering the fact that it was a trifluoride ~~to begin with~~ chemically,

and the axial ratios were comparable with the rare earth trifluorides.

G. General Discussion of the Two Trifluoride Structures

LaF_3 and all of the rare earth trifluorides up to and including EuF_3 were observed to precipitate from solution in the hexagonal form. In the cases of SmF_3 and EuF_3, the orthorhombic form was induced to appear when made at or treated to higher temperatures. CeF_3 failed to demonstrate distructuralism even after heating.

GdF_3, TbF_3, DyF_3, and TmF_3 were observed to precipitate from solution as the orthorhombic form and presumably all of the rare earth trifluorides from terbium through lutetium would also, given the proper conditions of excluding other positive ions such as ammonium and sodium. The hexagonal patterns in this region of the rare earths appeared only after high temperature treatment.

It has been observed that the hexagonal structures like CeF_3, SmF_3, and EuF_3 gave good powder patterns when precipitated from solution without any heat treatment other than drying ab. 100°C. The orthorhombic trifluorides, on the other hand, had to be heated before giving good patterns. Thus it might be possible for the hexagonal structure to form even though it was less stable than the orthorhombic structure, as it would nucleate and crystallize more readily. This might have been the case with the precipitation of the trifluorides of samarium and europium.

In the case of holmium trifluoride when an uncrushed chunk of the heated material was photographed, the powder patterns gave stronger hexagonal patterns than the crushed and powdered material. This could have been due to the fact that the surface was heated to a higher temperature and cooled more rapidly than the interior of the chunk; this is in

favor of the argument that the orthorhombic form was the low temperature stable form for these compounds.

It may be noted here that the hexagonal form ~~was~~ is a denser and apparently better packed structure than the orthorhombic form. This was best seen in comparing the average molecular volumes in the two structures as is shown in Table 23. These volumes were obtained from the unit cell volumes in Tables 5 and 18, by dividing them by 4 and 6, respectively.

Table 23

Average Molecular Volume in the Various Compounds for the Two Structures

	Hexagonal	Orthorhombic	% Difference
SmF_3	49.72 A^3	51.84 A^3	4.17
EuF_3	48.95 A^3	51.08 A^3	4.17
HoF_3	47.07 A^3	48.20 A^3	2.34
TmF_3	45.73 A^3	47.16 A^3	3.03

The HoF_3 and TmF_3 seem to be off considerably from the hexagonal series as can be seen in ~~the next figure~~ Fig. 17. SmF_3 reported by Oftedal (1929) seems to be off also.

The molecular volumes of the two series of structures were plotted and presented for comparison in Figure 17.

Regarding chemical stability of the various structures, one interesting observation was made. Hexagonal CeF_3 was heated in air at 400 to 600°C without any apparent change in the pattern except for the sharpening up a bit of some of the lines. When orthorhombic DyF_3 was heated in air to 500°C, it was completely converted to the sesquioxide. This was

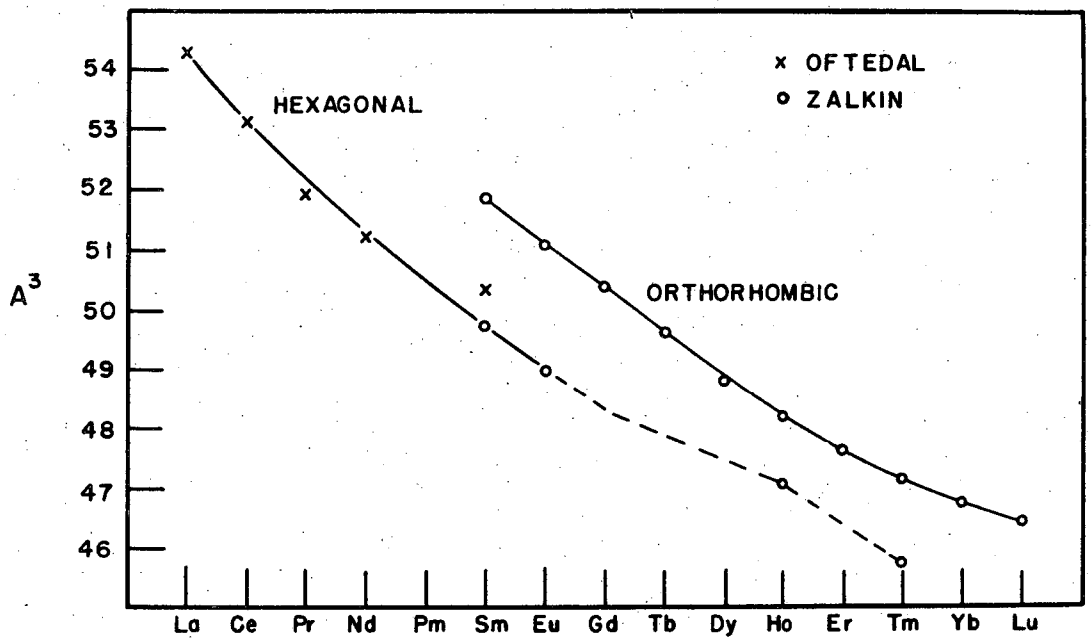

MU 1783

Fig. 17

Plot of the molecular volumes of the rare earth trifluorides.

probably not due so much to the difference in the two structures, but probably more ~~with~~ to the fact that as an ion decreases in size it becomes a weaker base, therefore cerium does not have as strong an attachment for oxygen as does dysprosium.

The main purpose of this research was to obtain the orthorhombic patterns for measurement, and no special effort was ~~done~~ made to determine the various stabilities. This discussion indicated roughly what further work would have to be done to more fully resolve the issues.

In summing up the relative stabilities of the two phases, it has been suggested that the hexagonal structure was a higher temperature form than the orthorhombic structure. In the region lanthanum through neodymium, the hexagonal structure was the room temperature stable form; in the region terbium through lutetium, the orthorhombic structure was the room temperature stable form. Samarium and europium fit in between the two groups and it cannot definitely be said which structure is the room temperature stable form; the hexagonal structure may form here mainly because it nucleates easier, leaving the orthorhombic form as the possible room temperature stable form.

H. Miscellaneous Non-trifluoride Compounds

1. Sodium-Holmium-Fluoride Compound (Hexagonal).-- As mentioned previously in the experimental section when sodium ion was introduced into the +3 holmium solution instead of ammonium ion, two new phases were observed in the powder patterns of the unheated material: a hexagonal phase and a cubic face centered phase. The hexagonal material was probably a sodium-holmium-fluoride compound of some unknown composition. Comparison with several mixed salts yielded no comparisons,

i.e., $NaLaF_4$ (Zachariasen 1948), β-$NaYF_4$ (Hund 1950[1]) and others. The powder pattern data for this material has been presented in Table 24; the face centered cubic lines were separated for discussion in the next paragraph. The cell constants for the hexagonal phase are:

$a = 8.862$ A $\quad c = 5.041$ A

$c/a = 0.5688$ $\quad$ Volume of one unit cell = 342.85 A^3.

The quality of the picture was fair, the lines tending to be a bit broad. The hexagonal phase showed indications of good crystallization, as evidenced by a certain amount of spottiness in the lines.

Table 24

Powder Pattern Data of a Sodium-Holmium-Fluoride Compound

Observed Intensities	hkl	$\sin^2\theta$* Calculated	$\sin^2\theta$* Observed
w	~~011~~ 001	.0516	.0512
m	110	.0669	.0666
m+	101	.0736	.0740
m	111	.1185	.1180
m	201	.1407	.1414
vw	210	.1560	.1552
vw	211	.2076	.2080
	002	.2065	
m+	301	.2522	.2527
vw	221	.3188	.3185
w	212	.3625	.3627
m+	401	.4060	.4073
	302	.4071	
w	103	.4870	.4871
w	312	.4945	.4965
w	113	.5316	.5314
vw	500	.5571	.5545
	203	.5538	
vw	402	.5609	.5634
m-	330	.6016	.6026
vw	501	.6087	.6036
w+	420	.6238	.6215
w	303	.6653	.6649
m	412	.6744	.6743
	421	.6754	
vw	223	.7319	.7324
vw	511	.7423	.7427
vw	313	.7543	.7542
w	520	.8690	.8690
m-	323	.8881	.8877
w	512	.8972	.8970
w+	413	.9326	.9324
vw	214	.9821	.9816

*Chromium K alpha x-rays (λ = ~~2.909~~ 2.2909 A)
a = 8.862 A; c = 5.041 A

2. Holmium Oxyfluoride (Face Centered Cubic).-- The face centered cubic phase was found to have far too big a cell constant to be anything like sodium fluoride; it was suspected of being either HoOF or $NaHoF_4$, both of which might have the fluorite structure. The intensities of the~~se two possible~~ lines of the two compounds were calculated (on the basis of a fluorite structure) and corrected for Lorentz polarization factor and multiplicity and then compared with the observed intensities. This treatment showed that this compound was probably HoOF. The observed and calculated data on the intensities and $\sin^2\theta$ ~~were placed~~ are shown in Table 25. The cell constant was found to be:

$$a = 5.523 \pm 0.003 \text{ A} \qquad V = 168.48 \text{ A}^3.$$

Calculated x-ray density of HoOF = 7.881 g/cc.

Table 25

HoOF, Calculated and Observed $\sin^2\theta$ and Intensities

$\sin^2\theta$*		$h^2+k^2+\ell^2$	$hk\ell$	Intensities		
					Calculated For	
Calculated	Observed			Observed	HoOF	$NaHoF_4$
.1289	.1291	3	111	s+	100	100
.1724	.1721	4	200	s-	30	2
.3447	.3442	8	220	s	52	68
.4738	.4732	11	311	s	47	46
.5187	.5162	12	222	w+	10	<1
.6888	.6883	16	400	m+	14	3
.8176	.8174	19	331	s	50	48
.8603	.8604	20	420	s-	33	30

*Chromium K alpha x-rays (λ = ~~2.909~~ 2.2909 A)

Other known oxyfluorides are:

AmOF (Templeton) a = 5.68 A
AcOF (Zachariasen 1949[1]) a = 5.955 A
PuOF (Zachariasen 1949[1]) a = 5.70 A
LaOF (Klemm and Klein 1941) a = 5.77 A
YOF (Templeton and Dauben) a = 5.51 A

3. An Ammonium Rare Earth Fluoride Compound (Cubic).-- Nowacki (1938) never was able to reproduce the cubic compound he described as yttrium trifluoride. Hund (1950[2]) tried to approach this cubic phase by mixing together varying quantities of β-$NaYF_4$ (cubic) and YF_3. As he increased the YF_3 content he got a series of cubic compounds with increasing cell constant approaching Nowacki's value; however, the cubic cell was not of the same type, and the densities began at values below Nowacki's density and increased far beyond.

In three cases ~~we found materials~~ patterns were obtained during ~~our~~ these investigations that had many similarities to Nowacki's cubic patterns. As was mentioned previously under the experimental section when holmium, erbium, and thulium were first precipitated and dried, they gave cubic patterns of the same type; when these materials were heated they were transformed into the trifluoride structures.

The material from the holmium precipitation was measured and indexed as a primitive cubic lattice with a = 5.81 $\pm$ 0.01 A. The thulium and erbium films were not measured but their cell constants were estimated not to vary from that for the holmium compound by more than the error limit. This was probably due to a very loose structure, and to the close value of the radii of the respective ions concerned.

The observed intensities obtained by visual estimation seemed to check fairly well with those reported by Nowacki for his cubic yttrium trifluoride pattern. This can be seen in Table 26 which presents Nowacki's intensities versus the ones obtained in the holmium film. The cell constant was much larger in our case than with Nowacki's (a = 5.664) which was probably due to his use of sodium ion and our use of ammonium ion. Nowacki probably had a mixed sodium-yttrium-fluoride salt of some unspecified composition.

Table 26

A Cubic Ammonium-Holmium-Fluoride Powder Pattern

hkℓ	$\sin^2\theta$* Calculated	$\sin^2\theta$* Observed	Observed Intensities	Nowacki's Intensities For Cubic YF_3**
100	.0389	.0383	w+	w
110	.0777	.0770	m	w
111	.1166	.1162	s+	s
200	.1554	.1552	m	m
210	.1943	.1948	w	vw-
211	.2332	.2311	w	vw-
		.2616		
220	.3109	.3108	s	vs
		.3409	vw	
221 300	.3497	.3493	w+	w
310	.3886	.3899	vw	vvw
311	.4275	.4277	s	s
222	.4663	.4651	w+	w+
		.4956	vw	
320	.5052	.5044	w-	vw-
321	.5440	.5432	w+	vw
		.5768	vvw	
400	.6218	.6218	w+	m-w
322 410	.6606	.6575	vvw	vvw
330 411	.6995	.7005	vvw	vvw
331	.7383	.7384	m+	m
420	.7772	.7768	m	m-w
421	.8161	.8148	vvw	vvw
332				vvw
422	.9326	.9330	m+	m

*Chromium K alpha x-rays (λ = ~~2.909~~ 2.2909 A)

**Copper K alpha x-rays

a = 5.81 ± 0.01

ACKNOWLEDGMENT

I am indebted to Dr. D. H. Templeton who originally suggested the problems discussed in this thesis, and who guided this research to its successful completion. I would also like to thank the following people for their help and assistance: Professor Brewer and Mr. Sawyer for their co-operation in preparing the samples of CeB_4, ThB_4, and UB_4; Mr. J. Wallman and Dr. L. B. Asprey for providing us with several samples of the rare earth trifluorides; Mrs. Lee Jackson for photographing many of the powder patterns; Mrs. Carol Dauben for some of the calculations; Mrs. Helena Rubin for photographing many of the powder patterns and for some of the calculations; and Dr. K. J. Palmer and Miss M. Ballantyne for the spectrometer record on UB_4.

This work was performed under the auspices of the U. S. Atomic Energy Commission.

REFERENCES

Allard, G. (1932). Bull. soc. chim. France 51, 1213.

Andrieux, J. L. (1929). Ann. chim. 12, 423.

Bertaut, F. and Blum, P. (1949). Compt. Rend., Paris, 229, 666.

Brewer, L., Sawyer, D. L., Templeton, D. H., and Dauben, C. H. (1951). Submitted to J. Am. Ceram. Soc.

Daane, A. and Baenziger, N. C. (1949). U. S. AEC Report ISC-53.

Ehrlich, P. (1947). Angew. Chem. 59, 163.

Hofmann, W. and Jäniche, W. (1936). Z. physik. Chem. B 31, 214.

Huggins, M. L. (1941). J. Chem. Soc. 63, 66.

Hume-Rothery, W., Rayner, G. V., and Little, A. T. (1942). J. Iron and Steel Inst. (London), Advance copy, March 15, 318.

Hund, F. (1950[1]). Z. anorg. Chem. 261, 106.

Hund, F. (1950[2]). Z. anorg. Chem. 263, 102.

Kiessling, R. (1949). Acta Chem. Scand. 3, 90.

Klemm, W. and Klein, H. A. (1941). Z. anorg. Chem. 248, 167.

Lipson, H. and Beevers, C. A. (1936). Proc. Phys. Soc. (London) 48, 772.

Lipson, H. and Petch, N. J. (1940). J. Iron and Steel Inst. (London) Advance copy, September.

McKenna, P. M. (1936). Ind. Eng. Chem. 28, 767.

Norton, J. T., Blumenthal, H., and Sindeband, S. J. (1949). J. Inst. Metals 1, 749.

Nowacki, W. (1938). Z. Krist. 100, 242.

Oftedal, I. (1929). Z. physik. Chem. 5 B, 272.

Oftedal, I. (1931). Z. physik. Chem. 13 B, 190.

v. Stackelberg, M. and Neumann, F. (1932). Z. physik. Chem. 19 B, 314.

Templeton, D. H. and Dauben, C. H. (1950). Unpublished work.

Tunnel, G. (1939). Am. Mineral 24, 448.

Vogt, T. (1914). Neues Jahrb. Mineral. Geol. 1914 II, 9.

Zachariasen, W. H. (1948). Phys. Rev. 73, 1104.

Zachariasen, W. H. (1949[1]). Acta Cryst. 2, 388.

Zachariasen, W. H. (1949[2]). Reported in Argonne National Laboratory Report ANL-4400 (September-November).